AD-A077 455 TENNESSEE UNIV KNOXVILLE F/G 11/9
RHEO-OPTICS OF SHEAR AND ELONGATIONAL FLOW OF LIQUID CRYSTALLIN--ETC(U)
OCT 79 Y ONOGI , J L WHITE , J F FELLERS N00014-77-C-0236
UNCLASSIFIED PSF-133 NL

| OF |
AD-
A077455

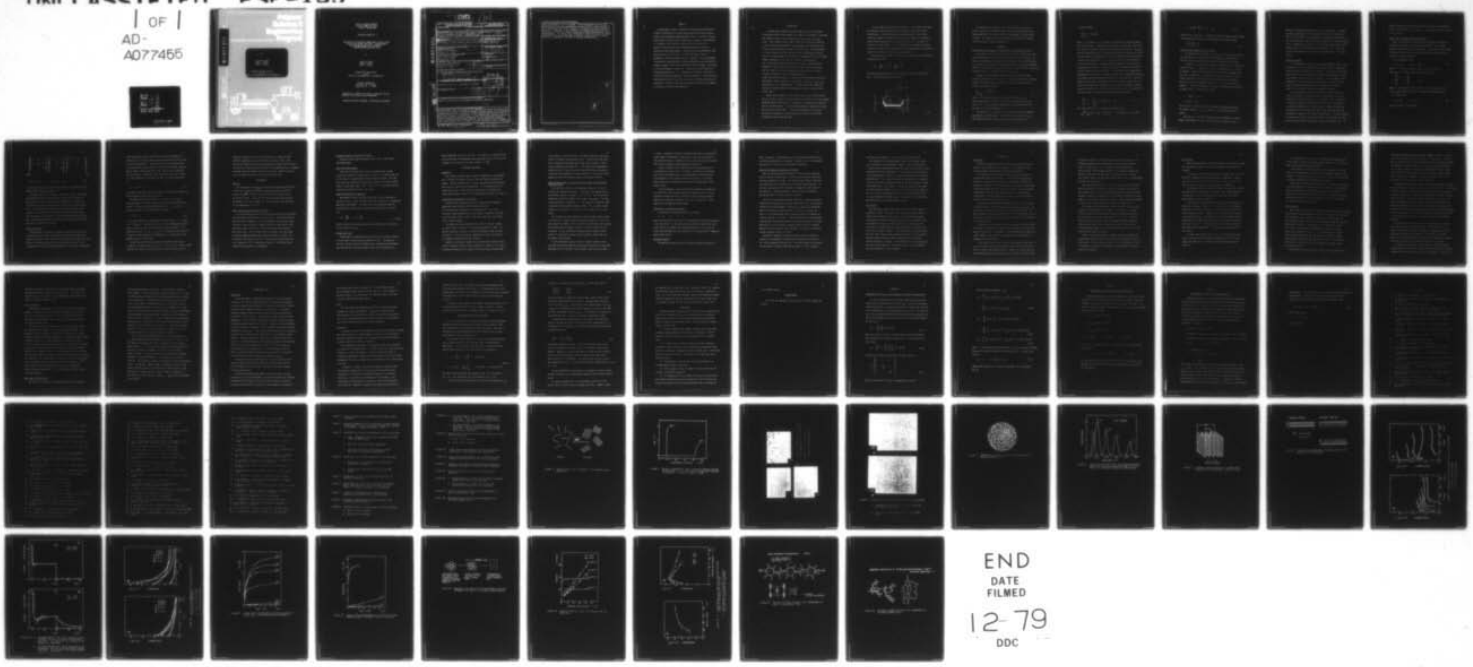

END
DATE
FILMED
12-79
DDC

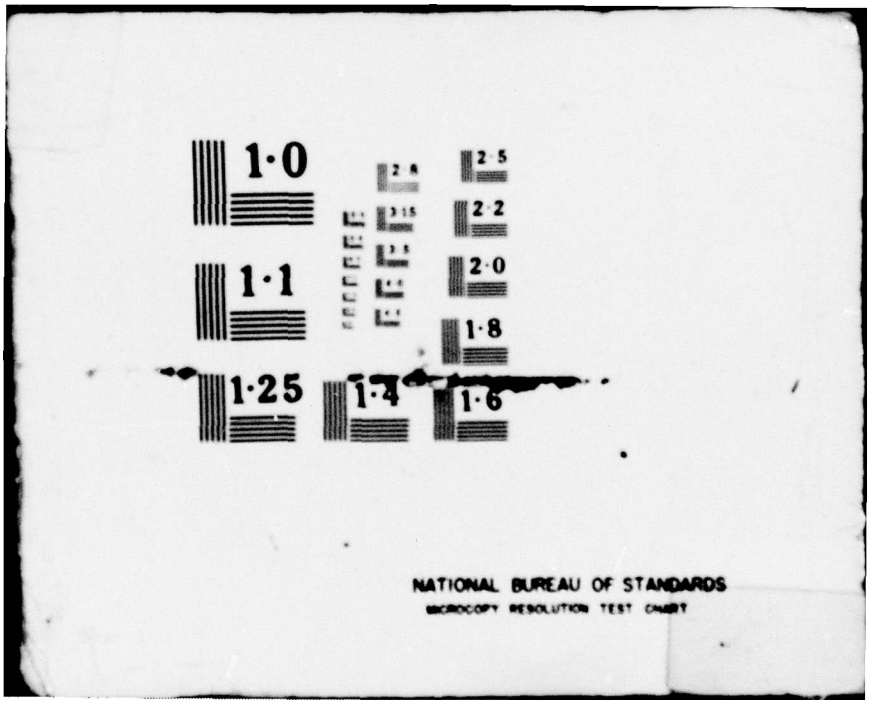
1·0
1·1
1·25
1·4
1·6
1·8
2·0
2·2
2·5
NATIONAL BUREAU OF STANDARDS
MICROCOPY RESOLUTION TEST CHART

by

Yoshihiko Onogi
James L. White
John F. Fellers

Prepared for Publication
in the
urnal of Non-Newtonian Fluid Mechanics

OFFICE OF NAVAL RESEARCH
Contract N00014-77C-0236
Task No. NR 356-639

TECHNICAL REPORT NO. 5

RHEO-OPTICS OF SHEAR AND ELONGATIONAL FLOW OF LIQUID CRYSTALLINE POLYMER SOLUTIONS: HYDROXYPROPYL CELLULOSE/WATER AND POLY-p-PHENYLENE TEREPHTHALAMIDE/SULFURIC ACID

by

Yoshihiko Onogi
James L. White
John F. Fellers

Prepared for Publication
in the
Journal of Non-Newtonian Fluid Mechanics

Polymer Engineering
University of Tennessee
Knoxville, TN 37916

AD A077455

DDC FILE COPY

SECURITY CLASSIFICATION OF THIS PAGE (When Data Entered)

REPORT DOCUMENTATION PAGE

READ INSTRUCTIONS BEFORE COMPLETING FORM

1. REPORT NUMBER: 5
2. GOVT ACCESSION NO.
3. RECIPIENT'S CATALOG NUMBER

4. TITLE (and Subtitle): RHEO-OPTICS OF SHEAR AND ELONGATIONAL FLOW OF LIQUID CRYSTALLINE POLYMER SOLUTIONS: HYDROXYPROPYL CELLULOSE/WATER AND POLY-p-PHENYLENE TEREPHTHALAMIDE/SULFURIC ACID.

5. TYPE OF REPORT & PERIOD COVERED: Technical 10-30-78 9-28-79

6. PERFORMING ORG. REPORT NUMBER: PSE Report No. 133

7. AUTHOR(s): Yoshihiko/Onogi, James L./White, John F./Fellers

8. CONTRACT OR GRANT NUMBER(s): N00014-77C-0236

9. PERFORMING ORGANIZATION NAME AND ADDRESS: Polymer Engineering, University of Tennessee, Knoxville, TN 37916

10. PROGRAM ELEMENT, PROJECT, TASK AREA & WORK UNIT NUMBERS: 346650

11. CONTROLLING OFFICE NAME AND ADDRESS: Office of Naval Research, 800 N. Quincy Street, Arlington, VA 22217

11 26 Oct 79

12. REPORT DATE: 10-26-79

13. NUMBER OF PAGES: 61

14. MONITORING AGENCY NAME & ADDRESS (if different from Controlling Office): NR Resident Representative, 325 Hinman Research Bldg., Atlanta, GA 30332

12 63

15. SECURITY CLASS. (of this report)

15a. DECLASSIFICATION/DOWNGRADING SCHEDULE

16. DISTRIBUTION STATEMENT (of this Report): Approved for Public Release; Distribution Unlimited

9 Technical rept. 30 Oct 78-28 Sep 79

DDC RECEIVED NOV 30 1979

17. DISTRIBUTION STATEMENT (of the abstract entered in Block 20, if different from Report): To be published in the J. Non-Newt. Fluid Mech.

18. SUPPLEMENTARY NOTES

14 PSE-133 TR-5

19. KEY WORDS (Continue on reverse side if necessary and identify by block number): Polymer Liquid Crystal, Birefringence, Anisotropic, Rheo-optics

20. ABSTRACT (Continue on reverse side if necessary and identify by block number): An experimental study is reported of the quiescent and flow birefringent characteristics of two liquid crystalline polymer solution systems, poly-p-phenylene terephthalamide (PPD-T) in sulfuric acid and hydroxypropyl cellulose (HPC) in water over a range of concentrations. It is shown, for the quiescent state, the dilute solutions are optically isotropic while the concentrated solutions consist of negatively birefringent domains. During flow at low deformation rates, moving domains are still seen. At higher deformation rates a homogenous

(over)

DD FORM 1 JAN 73 1473 EDITION OF 1 NOV 65 IS OBSOLETE
S/N 0102-LF-014-6601

346650

(cont)

and

highly birefringent fluid is obtained. The birefringence increases with concentration at constant deformation rate and exhibits a major increase as the liquid crystalline state is formed. The source of the birefringence is due to (1) anisotropy of polarizability of oriented macromolecules, (2) difference in refractive index of solvent and oriented macromolecules (form birefringence). The results are interpreted in terms of the level of polymer orientation which may be developed in flow for liquid crystalline polymer solutions as compared to solutions of flexible macromolecules.

SYNOPSIS

An experimental study is reported of the quiescent and flow birefringent characteristics of two liquid crystalline polymer solution systems, poly-p-phenylene terephthalamide (PPD-T) in sulfuric acid and hydroxypropyl cellulose (HPC) in water over a range of concentrations. It is shown for the quiescent state the dilute solutions are optically isotropic while the concentrated solutions consist of negatively birefringent domains. During flow at low deformation rates moving domains are still seen. At higher deformation rates a homogeneous highly birefringent fluid is obtained. The birefringence increases with concentration at constant deformation rate and exhibits a major increase as the liquid crystalline state is formed. The source of the birefringence is due to (1) - anisotropy of polarizability of oriented macromolecules, (2) - difference in refractive index of solvent and oriented macromolecules (form birefringence). The results are interpreted in terms of the level of polymer orientation which may be developed in flow for liquid crystalline polymer solutions as compared to solutions of flexible macromolecules.

INTRODUCTION

In recent years attention has been drawn to a class of polymer fluids which exhibit birefringence in a state of rest though in some ways they behave as normal liquids indeed often with a lower viscosity level. The existence of this order in the state of rest has resulted in those fluids being referred to as anisotropic as contrasted to isotropic systems which have no order in the rest state. These mesophase or liquid crystalline polymer systems include concentrated solutions (and in a limited number of cases melts) of polypeptides (1-9), p-linked aromatic polyamides (8-16) and other aromatic polycondensates (15, 17-21) and cellulose derivatives (9, 22-24). The mechanism of formation of these polymer liquid crystals seems largely associated with the rigidity of the macromolecules and the inability to pack a random arrangement of rods at moderate and high volume fractions.(See Figure 1). Flory (25) has developed a statistical thermodynamic lattice theory for concentrated solutions of rigid rods which predicts this transformation. In recent years, this model has received increased attention from Krigbaum and Salaris (20) and Flory and Abe (26).

Kwolek and her coworkers (10-12) found that fibers formed from wet and dry jet wet spinning of liquid crystalline solutions of p-linked aromatic polyamides possess high levels of orientation and mechanical properties even at low flow stresses. This has been observed in polyesters (17, 18) and cellulosics (23) as well. In a recent publication, we reviewed the earlier literature on liquid crystalline polymer fluids and the formation of fibers from them (27).

It would appear that molecular orientation is more readily developed and retained in these systems than in solutions or melts of flexible macromolecules. There have been some investigations of flow induced structural changes in polymer liquid crystals by Japanese investigators, notably Asada and Onogi (6, 7, 24) and Horio (15) who have made contributions to this subject. It is the purpose of this paper to present a report of research in our laboratories on the development of orientation during flow of liquid crystalline polymer solutions.

The two polymer systems of concern in this study are poly-p-phenylene terephthalamide (PPD-T)

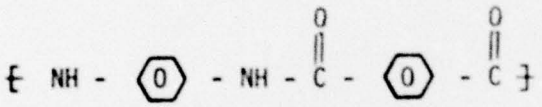

(I)

and the hydroxypropylcellulose ester (HPC) with degree of substitution four. This has an approximate structure

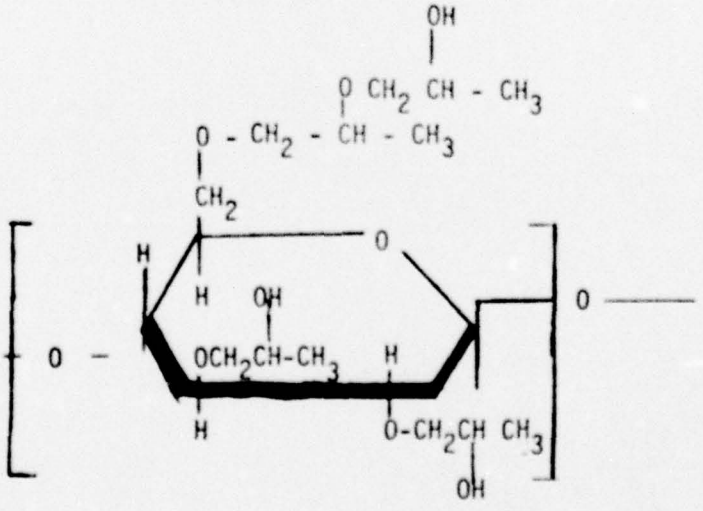

(II)

We investigate in particular the flow birefrinence of two different liquid crystal forming polymer solutions poly(p-phenylene terephthalamide)(PPD-T) in sulfuric acid and hydroxypropyl cellulose (HPC) in water. This paper continues the authors investigations of polymer liquid crystalline fluids (8,9,14,16,27).

BACKGROUND

Polarizability Anisotropy and Interpretation of Birefringence Levels

We attempt in this paper to determine the extent of molecular orientation developed during flow through measurements of birefringence. Before we can meaningfully proceed we must be able to relate birefringence to orientation. Birefringence in flowing polymer solutions may be related either to orientation or to geometry-refractive index difference (form birefringence) effects. We discuss each of these in turn.

Hermans and his coworkers (28) have shown that uniaxial fiber orientation measured by $\cos^2\theta$ (where θ is the angle between the preferred direction and the polymer chain axis) is related to the anisotropy of the polarizability through:

$$\frac{\overline{\Delta\alpha}}{\alpha_{||} - \alpha_{\perp}} = f = \frac{\overline{3\cos^2\theta - 1}}{2} \qquad (1)$$

where $\alpha_{||}$ is the polarizability along a polymer chain, $\alpha_{\perp}$ the value perpendicular to it and f is known as the Hermans orientation factor. $\overline{\Delta\alpha}$ is the difference between the mean polarizability along the fiber axis and perpendicular to it.

The value of $\overline{\Delta\alpha}$ in filaments is traditionally determined through measurements of birefringence. The 1880 theory of Lorentz (Lorentz-Lorenz equation) relates refractive index to the polarizability,

α, (20-31) through

$$\frac{n^2 - 1}{n^2 + 2} = \frac{4\pi}{3} \frac{N\rho}{M} \alpha \qquad (2)$$

where ρ is the density, N is Avogadro's number and M is molecular weight per structural unit. Lorentz (29) (pg 137-145, 305-308) notes that Eq(2) is limited to isotropic systems and cubic crystalline lattices. The problems associated with Eq(2) in two phase and anisotropic media were pointed out and analyzed by Rayleigh (32) as early as 1892 and has been discussed by more recent investigators such as Stein (33) for its application to crystalline polyolefins. Page and Adams (30) argue this formalism may be applied to anisotropic systems with n and α replaced by principal refractive indices and polarizabilities. Kuhn and Grun (34) independently developed and utilized this argument to predict the birefringent properties of deformed vulcanized rubber and Hermans et al (28) applied it to fibers. Gurnee (35) and later investigators used this concept to predict the intrinsic birefringence of polymer chains. Consider a completely oriented system of polymer chains. Again letting the subscript $\parallel$ mean parallel to the chain and $\perp$ to be perpendicular to the chain, we obtain:

$$\frac{n_{\parallel}^2 - 1}{n_{\parallel}^2 + 2} - \frac{n_{\perp}^2 - 1}{n_{\perp}^2 + 2} = \frac{4\pi}{3} \frac{N\rho}{M} (\alpha_{\parallel} - \alpha_{\perp}) \qquad (3)$$

For small values of $n_{\parallel} - n_{\perp}$, we may reduce Eq (3) to

$$\left(\frac{6\bar{n}}{\bar{n}^2 + 2}\right)^2 (n_{\parallel} - n_{\perp}) = \frac{6\bar{n}}{(\bar{n}^2 + 2)^2} \Delta^\circ = \frac{4\pi}{3} \frac{N\rho}{M} (\alpha_{\parallel} - \alpha_{\perp}) \qquad (4a)$$

$$\Delta^\circ = \frac{2\pi}{9} \frac{N\rho}{M} \frac{(\bar{n}^2 + 2)}{\bar{n}} (\alpha_{||} - \alpha_{\perp}) \qquad (4b)$$

Based on Eqs (1) and (4), the Hermans orientation factor may be related to the measured and intrinsic birefringence of filaments through:

$$f = \frac{n_1 - n_2}{n_{||} - n_{\perp}} = \frac{\Delta n}{\Delta^\circ} \qquad (5)$$

Intrinsic Birefringence of PPD-T and HPC

To proceed we must evaluate $\alpha_{||}$ and $\alpha_{\perp}$ for the PPD-T and HPC chains. This may be done as suggested by various authors by considering an extended chain structure and adding bond polarizabilities (35, 36).

In Appendix 1, we detail the method of computation of Δ° from bond polarizabilities. A computation using this method for PPD-T is given in Appendix 2 where the bond polarizabilities of Bunn and Daubeny (36) are used. In Appendix 3, we attempt to estimate Δ° for HPC. The unknown orientation of the propylene oxide substituents in Formula II does not allow for a meaningful prediction of Δ° using the methods of Appendix 1. We have estimated it from data on oriented films published by Samuels (37). We obtained the results

$$\Delta^\circ \quad (\text{PPD-T}) = 0.37$$

$$\Delta^\circ \ (\text{HPC}) = 0.038$$

The values of Δ° are for crystals and should be appropriately lower for polymer solutions, i.e. $\phi_p \Delta^\circ$ where ϕ_p is the volume fraction of polymer.

The value of Δ° for PPD-T should be directly comparable to experimentally measurements on highly oriented fibers (though not for HPC

because birefringent data were used in its determination). Konopasek and Hearle (38) report Δn for oriented fibers with the structure of PPD-T to be 0.45 which is troublesome as it exceeds the theoretical Δ°. Possible difficulties are (i) the lack of additivity of bond polarizabilities in condensed ring systems, (ii) inaccurate representation of the internal field, (iii) inaccurate bond polarizabilities. Stein (33) has discussed problems of this type in the evaluation of Δ° for polyolefins.

Form Birefringence

In two component systems, one must evaluate whether there is birefringence due to the two components possessing different refractive indices and being anisotropically distributed. The theory of such form birefringence is due to Rayleigh (32) and has been extended by various investigators since that time (31, 39, 40). A recent example of the importance of form birefringence has been Folkes and Keller's (41) study of extruded filaments of block copolymers which contain a parallel of cylinders of one phase suspended in a second.

In the present paper we are concerned with polymer solutions. There has long been a concern with form birefringence arising from orientation in flowing polymer solutions (42-44). This is the result of studies showing the birefringences of these systems exhibiting a significant dependence on solvent (42, 43). However, theoretical considerations of this effect have been limited to dilute solutions and models of dumbbells and isolated flexible chains. We have attempted to estimate the maximum form birefringence of PPD-T and HPC solutions using the Rayleigh-Wiener theory (32, 39, 41) for parallel rods. The

predicted values are of order 20 percent of the intrinsic birefringence of the solution taken as $\phi_p \Delta^\circ$, where ϕ_p is the volume fraction of polymer in the solution.

Stress Field in Elongational and Shear Flow

There is an extensive literature on the rheological properties of concentrated solutions of flexible polymer chains. These systems generally respond as isotropic viscoelastic fluids and the stress fields in flows of interest may be expressed in terms of non-linear viscoelastic constitutive equations.

In an elongational flow:

$$v_1 = v_1(x_1) \qquad v_2(x_2) = v_3(x_3) \tag{6}$$

where 1, 2, 3 are an orthogonal frame. The resulting stress field $\underline{\sigma}$ for an isotropic viscoelastic fluid is (45)

$$\underline{\sigma} = \begin{vmatrix} \sigma_{11} & 0 & 0 \\ 0 & 0 & 0 \\ 0 & 0 & 0 \end{vmatrix} \qquad \sigma_{11} = \frac{F}{A} \tag{7}$$

where F is the applied tension and A the cross-sectional area. σ_{11} in the steady state depends upon the elongational deformation rate.

In a shear flow

$$v_1 = v_1(x_2) \qquad v_2 = v_3 = 0 \tag{8}$$

The stress field is of form (46)

$$\underset{\sim}{\sigma} = \begin{vmatrix} \sigma_{11} & \sigma_{12} & 0 \\ \sigma_{12} & \sigma_{22} & 0 \\ 0 & 0 & \sigma_{33} \end{vmatrix} = \begin{vmatrix} \sigma_{33} & 0 & 0 \\ 0 & \sigma_{33} & 0 \\ 0 & 0 & \sigma_{33} \end{vmatrix} + \begin{vmatrix} N_1 + N_2 & \sigma_{12} & 0 \\ \sigma_{12} & N_2 & 0 \\ 0 & 0 & 0 \end{vmatrix} \quad (9)$$

where

$$N_1 = \sigma_{11} - \sigma_{22} \qquad N_2 = \sigma_{22} - \sigma_{33} \quad (10)$$

N_1 and N_2 are the principal and second normal stress differences which depend on the steady state shear rate.

The above forms are for isotropic viscoelastic fluids. There have been rheological theories developed for liquid crystals notably by Frank (47) and Ericksen (48) for static deformations. Theories of flow of liquid crystals are presented by Leslie (49, 50) and Ericksen (51). These theories are intended for low molecular weight liquid crystals. Their predictions for steady flows are much more complex than viscoelastic fluid theory and complex boundary effects arise (52-54). Some experimental studies on low molecular weight liquid crystal bear out such complexities (55, 56).

Flow Birefringence

The development of molecular orientation during flow of solutions of macromolecules has been investigated using flow birefringence for generations (57-59). Most efforts have been directed at dilute solutions and have involved biological and rigid macromolecules and to a more limited extent flexible hydrocarbon polymers (vinyl polymers, polydienes).

These studies have aimed at determining individual macromolecule characteristics including rotary diffusion constants and chain length for rigid macromolecules. Investigations for concentrated polymer solutions and melts have focussed on flexible chains where Lodge (60) and Philippoff (61-64) among others (65 - 68) show the development of birefringence is governed by the 'rheo-optical law' which relates it to the difference in principal stresses σ_i existing during flow, i.e.

$$n_i - n_j = C(\sigma_i - \sigma_j) \tag{11}$$

This behavior has been justified in terms of the theory of networks of flexible polymer chains (35, 60, 69, 70).

Oda, White and Clark (71) note it is implicit in the theory of birefringence in flexible polymer chain networks that the stress-optical C constant should be proportional to $(\alpha_{11} - \alpha_1)$ and to Δ°. In uniaxial extension, it follows from Eq (11) that

$$f = \left(\frac{C}{\Delta^\circ}\right) \sigma_{11} \tag{12}$$

is to a good approximation independent of polymer type. C/Δ° is about 2×10^4 Brewster. They verify this for on-line birefringence measurements on fiber spinlines and vitrified polystyrene filaments. The proportionality of C to $(\alpha_{11} - \alpha_1)$ and Δ° also explains Philippoff and Tornquist's (64) finding of the dependence of C on the length of the pendent group on a vinyl chain.

Polymer liquid crystalline fluids are characteristically birefringent in the state of rest (1-3, 8-13, 16, 22, 23, 27). However, there have been few studies of the rheo-optics of these polymer solutions.

Indeed as noted earlier only the investigations of Asada and Onogi and their coworkers (6, 7, 24) and Horio (15) may be cited. These authors have reported on the flow birefringence of both dilute isotropic solutions and liquid crystalline solutions of polypeptides (6, 7), aromatic polyamides (15) and hydroxy propyl cellulose (24). However, their results are rather qualitative and limited to shear flow.

EXPERIMENTAL

Materials

The two polymers used were poly-p-phenylene terephthalamide (PPD-T) in the form of DuPont Kevlar® and hydroxypropylcellulose (HPC) as Hercules Klucel® L. The PPD-T was dissolved in 100% sulfuric acid and the HPC in water. These are the same two polymer solution types considered in our earlier paper (9). All experiments were carried out at room temperature (ca. 23°C).

Optical Microscopy of Quiescent Solutions

A Leitz-Ortholux polarizing light microscope was used to investigate the birefringent characteristics of the systems. The sample thickness was controlled in two ways. For the measurement of the thicker sample solutions, Fisher Scientific Littmann Slides (for fungus mounts) were used with a glass cover slide. These slides possess depressions of 600 microns (μm). For the thinner sample solutions, cells were made by pressing samples between glass plates separated by a spacer. The thickness of the spacer was 100 μm. The microscope sample holder had a hot stage with ± 0.5°C temperature regulation. Transmitted light intensity was measured with a photometer.

Absorption Spectra on Quiescent Solutions

Absorption spectra were determined with a Cary 17 double beam spectrophotometer.

Shear Flow Birefringence

Shear flow experiments were carried out between glass plates using teflon spacers of thickness 56 μm or 88 μm. The plates were set on the stage of a compensating polarized light microscope. The upper glass plate was drawn at various constant velocities to obtain a wide range of steady shear rates ($10^{-1} \sim 10^{1}$ sec $^{-1}$). The shear flow birefringence was measured in the '1-3' plane.

Shear Flow Rheological Properties

Measurement of shear flow principal normal stress difference N_1 and shear stress σ_{12} were obtained for the HPC solutions on a Rheometrics Mechanical Spectrometer. The shear stress was determined from the torque M and the normal stress difference through the thrust force F (72)

$$\sigma_{12} = \frac{3M}{2\pi R^3} \quad ; \quad N_1 = \frac{2F}{\pi R^2} \qquad (13\ a,b)$$

Similar studies on PPD-solutions have been carried out in our laboratories by Aoki et al (8).

Elongational Flow

Elongational flow experiments were carried out by gravity spinning in which sample solutions were extruded from a die. The apparatus used was a Harvard infusion/withdrawal pump. Retardation measurements were carried out by setting a Olympus polarizing microscope with a

Berek compensator across the spinline. The diameters of filaments along the spinline were also determined from photographs taken with the aid of a camera using a close-up lens (Micro Nikkon f = 55mm).

QUIESCENT SOLUTIONS

Appearance

The solutions studied showed a range of appearances to the unaided eye. The PPD-T anisotropic solutions are dark brown and essentially opaque. The HPC solutions have a striking appearance exhibiting colors which vary as a function of concentration. At a concentration of 53 weight percent (wt. %) the HPC/H_2O solutions are an iridescent red orange which changes to blue as the concentration increases to 70 (wt. %).

Transitions to Anisotropic Fluid Phases

The polarizing microscope was used to determine the conditions under which the solutions studied became anisotropic.
All solutions were isotropic at low concentrations. Over a concentration range characteristic of the polymer, a transition occurred to an anisotropic phase in which light came through the cross polars. This is shown in Figure 2.

The phase transition characteristics differ for the two systems. In case of PPD-T, it occurs in a very narrow composition range. For the HPC solutions, it occurs in a wider concentration range as shown in Figure 2. The log I/I_o versus concentration curves for the PPD-T are steeper than those of the HPC solutions.

Generally, anisotropic polymer liquid crystalline solutions transform to isotropic liquids as they are heated up. When a 9.5 wt.% PPD-T solution was heated on a hot stage of the polarizing microscope under

cross polars at a rate of 5 min/C°, the phase transition from anisotropic to isotropic was observed at 57°C. On the other hand, when this solution was cooled down at the same rate (5 min/C°), liquid crystal formation occurred at 38°C. This supercooling phenomenon is characteristic of liquid crystalline polymer solutions, and was observed for other polymer (8) systems except HPC. In the case of HPC aqueous solutions, HPC molecules begin to precipitate at 38°C.

Detailed Observations of Liquid Crystalline Phases from Polarized Light Microscopy

The solutions of PPD-T in the two phase region (9 ~ 9.5 wt.%) display small globular structures. (Figure 3a) The average size of the globular particles is about 5 μm (5×10^4 Å). The particles are spherulites exhibiting a Maltese cross under cross polars. The sign of the spherulites is negative, i.e., the tangential refractive index is greater than the radial refractive index. At a slightly higher concentration, aggregates of spherulites with diameter of 50 μm are formed.

The structure of single phase PPD-T and of polymer liquid crystalline solutions in general cannot be characterized easily. This is in part becuase the features of the solutions are affected by the shearing force applied when the sample solution is poured into the cell for microscopy. As the orientation relaxation time of polymer liquid crystals is quite long, characterization requires several days for the sample to equilibrate.

In the single phase structure there is complex 'domain' microstructure consisting of what may be aggregated spherulites (Figure 3b). Individual units of the PPD-T liquid crystals seem to be very small

(< 10μm). Threadlike structures resembling those seen in low molecular weight nematic thermotropic liquid crystals (73, 74) are observed if the anisotropic phase is melted at 90°C to form an isotropic liquid and then slowly cool down to room temperature (Figure 3c).

The HPC solutions do not show a distinctive morphology until a concentration of order 40 wt.% is reached. Above this concentration very small birefringent particles and aggregates of these particles are suspended in the isotropic phase (See Figure 4a). In the two phase region the HPC solutions show very fine structure that is not found in PPD-T.

In the anisotropic region with the HPC concentration between 53 wt.% and 70 wt.% the solutions exhibit an iridescent color. At concentrations higher than 70 wt.% the HPC solutions exhibit domains at spherulitic structures of dimensions 20 ∿ 80 μm (Figure 4b). These spherulites are negatively birefringent.

Implications of Spherulite Structure

The existence of negative spherulites indicates

$n_\theta > n_r$ or $\alpha_\theta > \alpha_r$

where the subscripts θ and r refer to the tangential and radial directions in the spherulite. As the polarizability along the length of the PPD-T and HPC chains are greater than that perpendicular to it, we may conclude these macromolecules are oriented in a circumferential or tangential manner (See Figure 5).

Absorption Spectra

The absorption spectra of the HPC liquid crystalline structure is

shown in Figure 6. The maximum peak of the absorption spectrum shifts as the HPC concentration is increased. The peak shift is also observed when the cell is inclined to the measuring light beam.

Cholesteric Character and Absorption Spectra

Many low molecular weight thermotropic liquid crystals have been found to have an internal twist in their structure and are classified as being cholesteric (73, 74). This internal twist leads to selective and directional light scattering and to optical rotary character. It has been associated with the existence of asymmetric carbon atoms in the molecules. The name cholesteric derives from the cholesteryl derivatives which strikingly show this character.

The pitch of low molecular weight cholesteric structures has been determined by Ferguson (75) and later investigators (76, 77) analyzing diffraction of electromagnetic radiation as a function of wavelength. When the orientation of the cholesteric structure is uniform, the pitch 'p' can be determined from the maximum peak of the apparent absorption spectrum. The pitch is indeed proportional to the wavelength corresponding to maximum diffraction or absorption intensity. We have been able to use this method to compute pitch for the HPC solutions. Generally this was found to vary from 5200 Å to 2600 Å as the concentration increases from 53 to 70 wt.%.

Cholesteric character in polymer solutions has been previously reported for polypeptides including $P_{\gamma}BLG$ by Robinson (1-3) and for HPC in H_2O by Werbowyj and Grey (22). The latter authors using optical rotation report a value of 3600 Å at 66 weight %. PPD-T solutions

would seem to be nematic, i.e. they possess no internal twist.

The ordering of the macromolecules within the helicoidal cholesteric structure is of considerable interest. The observed pitch 'p' is several orders of magnitude larger than that of any internal helical structure within the macromolecule. It would thus seem obvious that it may correspond to a twist in a direction perpendicular to planes of macromolecules. This is the view taken by Robinson and his coworkers (1-3) for solutions of polypeptides and it should also apply to planes of macromolecules. (See Figure 7). Bernal and Fankuchen (78) argue in investigations of tobacco mosaic virus suspensions, which appear to exist in a liquid crystalline form, that the rigid rod viruses exist in a two dimensional hexagonal array. A similar view is expressed by Robinson et al (2) for the polypeptide systems.

Wall Effects

We have found a sample size effect in our 'absorption' spectra experiments on HPC. This leads to the conclusion that the walls influence the orientation of the layers. From experimental studies using sample cells with a range of thicknesses, the structure of the anisotropic HPC solutions in narrow cells can be concluded to be a cholesteric structure with its planes parallel to the plane of the cell walls as shown in Figure 8. On the other hand, from the studies with cells with larger distances between the walls it was found that the wall planes of the cell play an important role in forming a uniform cholesteric structure. In the thicker cell the structure near the walls (within about 120 μm from the surface) is highly ordered, but in the inner part is less ordered.

SHEAR FLOW

HPC Results

Shear flow experiments on HPC solutions were carried out using parallel glass plates with 88 μm spacers. The isotropic, single phase anisotropic and two-phase solutions were examined.

The isotropic solution showed a steady state birefringence in seconds after applying steady shear. The birefringence decayed to near zero in seconds after cessation of steady flow. However, for anisotropic solutions, it took some minutes to achieve a steady state birefringence after applying a steady shear flow. This was true for single phase anisotropic and two-phase systems. The build-up of birefringence in steady shear for each type of solution is shown in Figure 9 (a) and (b) and 10 (a) and (b).

The decay of birefringence following cessation of flow is shown in Figure 10 and 11 for the isotropic and anisotropic solutions. For the isotropic solution this occurred in less than one minute. For the anisotropic systems about 15 percent of the birefringence still remains after 30 minutes, even though the stress again totally relaxes in a minute or less.

The anisotropic solutions inevitably have some preferred orientation which is created during sample loading between glass plates and does not relax easily. The shapes of birefringence build-up depend on sample loading. The time scale is always several minutes which is dependent on the shear rate.

In the case of the 55% HPC solution (single phase anisotropic) at 0.1 sec^{-1} shear rate, well defined birefringence only became observable 3.5 minutes after applying shear. Before this time no well defined observation was possible because of the domain structure of the

anisotropic solution. For single phase anisotropic solutions, birefringence overshoot could be observed in a range of shear rates as shown in Figure 9 (b), i.e., a steady state was obtained after passing through a birefringence maximum. The overshoot maximum time depends on the shear rate and shifts to shorter times as the shear rate becomes larger. At shear rates higher than 2.4 sec^{-1}, birefringence overshoot was not observed.

The birefringence build-up is shown in Figure 9 (a) for the two-phase anisotropic HPC solutions in which the isotropic and the anisotropic phase coexist. No birefringence overshoot was detected for the two-phase solutions as found for the single phase anisotropic solutions. However, it also took a long time to obtain a steady state birefringence as in the case of single anisotropic solutions (Figure 9 (b)).

The steady state birefringence of HPC solution of various concentrations is plotted against shear rate, $\dot{\gamma}$, in Figure 12. Isotropic solutions show a linear relationship between the birefringences and the shear rate in the range studied here ($\dot{\gamma} = 0.1 \sim 10$). For anisotropic solutions the steady state birefringence increases logarithmically against shear rate at shear rates between 0.3 and 4.0 sec^{-1}. The birefringence levels off at a shear rate of about 10 sec^{-1} for the single phase anisotropic solutions.

There is a striking increase in steady state birefringence with concentration near the critical concentration for formation of anisotropic phase. This is shown in Figure 12. At a shear rate of 10 sec^{-1} Δn increases by an order of magnitude as the concentration increases from 40 to 50 percent.

PPD-T Results

Shear flow measurements of PPD-T anisotropic solution were carried out using thinner spacers of 56 μm thick because of its higher birefringence.

As solutions of PPD-T in 100% H_2SO_4 are colored brown, it is very difficult to measure the birefringence with a compensator. Special care must be used as the anisotropic solutions show a distinct fine domain structure which makes the measurement more difficult.

The behavior of PPD-T isotropic solutions in shear flow is almost the same as that of HPC isotropic solutions. The steady state birefringence has a linear relationship with shear rate in the whole range studied as shown in Figure 13.

The structure of anisotropic PPD-T solutions (10%) sheared at a shear rate less than 0.09 sec^{-1} still show distinct fine polydomains even after a 20 minute flow period. It was almost the same as that of the unsheared solution. Therefore, no birefringence was observed in low shear rate flow. At higher shear rates birefringence became observable after a long induction period; it took seven minutes at a shear rate 0.18 sec^{-1}. The observed values were almost the same as the steady state birefringence. No smaller values were observed in this system.

At shear rates greater than 3.7 sec^{-1}, the retardation of the sample solution was greater than that observable with our 10 order compensator (6000 μm). This means the birefringence was greater than 0.11.

The retardations of 14% of PPD-T solution sheared between glass plates with 50 μm spacers were also greater than 6000 μm. No measurements could be made in these conditions.

From Figure 13 it may be seen that as one proceeds from the isotropic to the anisotropic state there is an enormous increase in birefringence. Clearly at any shear rate, the 10% solution shows more than one order of magnitude of birefringence over the 8%.

Birefringence relaxation after cessation of steady shear flow was also measured for the 10% anisotropic PPD-T solution. It was observed that the birefringence values became obscured by light scattering effects after three minutes from the cessation of steady shear and the observable birefringence did not decrease as rapidly in this period as in the HPC anisotropic solutions.

HPC Discussion

Basic studies of the liquid crystalline structure of HPC-H_2O solution were reported by Werbowyj and Grey (20) and by ourselves (8). Recently, the deformation of HPC cholesteric structure in shearing flow have been studied by Asada et al (24) using the apparent absorption spectrum measurement (9, 75-77). They suggest the HPC cholesteric structure can flow at low shear rates and transforms to a nematic structure at shear rates higher than 1.30 sec^{-1}. The irridescent color caused by the selective reflection of light were also observed in steady state shearing flow shear rates lower than 4.7 sec^{-1}. The intensity of cholesteric irridescent color was confirmed to decrease as the shear rate increased.

Birefringence overshoot over much larger time scales than stress

overshoot was observed at low shear rates ranging from 0.1 to 0.60 sec^{-1} for the single phase anisotropic solution. (Figure 10(b)). This may mean at the beginning of shear deformation the large cholesteric domains are deformed by localized high shear. This causes the birefringence of the sample solution to increase to a higher value than the steady state and then to slowly decay to a steady state as a 'dynamic equilibrium' structure is achieved. At shear rates higher than 1.2 sec^{-1} the effect of localized shear is almost negligible.

Birefringence relaxation of HPC solutions after cessation of steady flow is plotted as a function of time in Figure 11(a) and (b). For isotropic solutions, the birefringence became almost zero within 1 minute after cessation of shear flow. However, the birefringence relaxation of anisotropic solutions is very slow compared with isotropic solutions. Recovery of cholesteric irridescent color came to be observable as the birefringence decreased. This recovery of cholesteric structure after cessation of shear was also found by Asada et al (24) using the technique of light spectroscopy. This structural change of the HPC liquid crystal is a recovery of the cholesteric structure from the oriented nematic structure.

The observations of the quiescent state indicated the existence of oriented solid layers along boundaries. The existence of such layers in flow would obviously be important in interpretation of both rheological and rheo-optical behavior. The existence of boundary layers in low molecular weight liquid crystals was suggested by various investigators (54-56) for low molecular weight liquid crystals.

In summary we observe that in the quiescent state the one-phase solution consists of cholesteric liquid crystalline structures existing in domains with oriented structures at solid boundaries. In flow the

cholesteric structure is transformed to an oriented nematic structure and domain boundaries disappears. (See Figure 14). The fate of the boundary layers is not known. The oriented nematic state relaxes very slowly to reform the isotropic state.

PPD-T Discussion

Birefringence measurements of PPD-T solutions were very difficult because of the high intrinsic anisotropy of polymer molecule and of the color of PPD-T/H_2SO_4 solution. This is especially the case for anisotropic solutions where light scattering by the domain structure increases the difficulties.

In the case of HPC, the mechanism of structural change by shear was from cholesteric domains to an oriented nematic structure. The mechanism of PPD-T anisotropic solution can be considered to be from a nematic structure having small domains to a homogenous oriented nematic structure (Figure 14). In the lower shear rate range (less than 0.1 sec^{-1}), no striking change of domain structure of 10% of PPD-T was found by microscopic observations and no birefringence values were measured because of the scattering effect of the heterogeneity of the structure. This means these domain are stable for low shear and appear to flow under mild shearing. The oriented nematic structure of 10% PPD-T was obtained only in the steady state at shear rates of more than about 0.2 sec^{-1}! The structure of the oriented nematic state was very homogenous under microscopic observations, i.e., no structures other than stream lines were observed.

Magnitudes of Birefringence

The intrinsic anisotropy of the polymers used in this study has

been discussed earlier in this paper. The theoretical intrinsic birefringence Δ° of PPD-T uniaxially oriented crystal is 0.37. Those for HPC uniaxially oriented crystal and amorphous region are 0.04 and 0.02, respectively. The values for the solutions are $\phi_p\Delta^\circ$ or 0.04-0.05 for a 10% PPD-T solution and about 0.01 for the HPC solutions. Form birefringence effects may raise this value another 20%. These values of HPC are seen to be reasonable compared with the birefringence values obtained by shear experiments. However, the birefringence of PPD-T anisotropic solutions is too large compared with the calculated maximum values. Theoretically, considering density differences, $\phi_p\Delta^\circ$ could be as high as 0.066 using our value of Δ° and 0.085 if we were to take Δ° to be 0.40. Form birefringence could raise this to 0.1. This would make our 10% solutions completely oriented.

Let us turn to the problems that exist in the calculation of $\phi_p\Delta^\circ$ which might place our estimates of this for PPD-T in error. The Bunn-Daubeny polarizabilities (36) as suggested by Stein (33) may underestimate Δ°. It is also possible that the bond polarizabilities additivity discussed in Appendix 1 may not be valid for highly aromatic systems. This could explain the discrepancy with Konopasek and Hearle's fiber birefringence. Other problems exist for the solutions. One difficulty involves the estimation of form birefringence levels. The Rayleigh - Wiener theory is undoubtedly much too crude. Another difficulty arises in that the PPD-T probably becomes a poly-electrolyte in solution and has a layer of HSO_4^- associated with it. The influence of such structure on both $\alpha_{||} - \alpha_{\perp}$ and form birefringence is not obvious.

ELONGATIONAL FLOW

HPC Results

The birefringence in elongational flow of the isotropic and the anisotropic HPC solutions were measured by a solution spinning method. In the end, gravity was used because it proved very difficult to obtain a stable flow of polymer solutions on a rotating roll. A distinct difference between isotropic and anisotropic solutions was observed in the profiles of the spinline. These profiles showed no extrusion rate dependence. For the isotropic solution the spinning solutions continue to deform along the length of the spinline. However, for the anisotropic solution all changes in diameter of the filament occurred within several centimeters from the die. If we assume incompressibility of the solutions, the velocities of flow along the spinline may be calculated from these profiles. These are plotted as a function of distance from the die in Figure 15. The elongation rate of the isotropic solution (30%) was about 1.90 sec^{-1} for a 50 cm take-up and 2.74 sec^{-1} for a 100 cm take-up, at a distance of 20 cm from the die. For the anisotropic solution (55%) all velocity gradients abruptly go to zero within 5 cm from the die, and almost no velocity change occurs after this point.

The observed on-line birefringence of isotropic solutions of HPC (30%) is shown in Figure 16a as a function of the distance from die. The birefringence rises to a steady state value within approximately 75 cm from the die exit.

On-line birefringence measurements of HPC anisotropic solutions were carried out in the same manner. No domain structures were observed. The measured birefringence of 50% and 55% HPC anisotropic solutions at various positions on the spinning line are plotted as a function of

the distance from the die in Figure 16b. The birefringence values are considerably larger than for the 30% solution. They increase to a maximum at about 2.5 cm from nozzle. At lower positions in the spinline the birefringence becomes smaller.

PPD-T

On-line birefringence measurements of PPD-T solutions were also attempted using the same apparatus. Owing to the large intrinsic anisotropy and light absorption by colored sample solutions, and moreover, to the large diameter of the spinline solutions, the retardation could not be observed by using a 10 order compensator.

Discussion

As shown in Figure 15 the elongation rate of HPC anisotropic solutions was almost constant in a range between 5 cm and 15 cm from the nozzle. On-line birefringence values in this range were measured and reached a constant value as also shown in Figure 16b.

The stationary birefringence of elongational flow can be expressed as a function of elongation rate. A similar function for shear can also be expressed. If the birefringence is taken to indicate the level of orientation developed, a comparison of elongational to shear flow reveals elongational flow is about three times more effective at the same deformation rate.

In general, it takes a long period to obtain a stationary state after applying steady shear to liquid crystalline polymer systems. Consequently, in the case of elongational flow of a fluid emerging from a die, it is difficult to interpret the birefringence. Very high values of birefringence of anisotropic solutions were measured on the spinline. Moreover, a maximum birefringence was observed at a

position near the die. The maximum orientation was obtained within a short time after emerging from the die. The elongational rate at this deformation in the case of 100 cm take-up of 55% HPC solution is estimated to be more than 1.2 sec^{-1} and for one 50 cm take-up to be more than 5.4 sec^{-1}.

In terms of $\Delta n/\phi_p \Delta^\circ$ which is the Hermans orientation factor, Eq (5), the values are less than 0.01 for the isotropic solutions. For the 55% HPC solution the value is remarkably high in the range 0.3 to 0.5.

BIREFRINGENCE-STRESS RELATIONSHIPS

It is very interesting to know the relationship between mechanical responses and optical properties of polymer liquid crystals in flow. This relationship has been studied for flexible polymer chains and is the rheo-optical law developed for flexible polymer chains relating birefringence to stress through Eq (11).

The principal stress difference in shear flow is obtained from N_1 and σ_{12} values obtained at the same shear rate in the Mechanical Spectrometer. In the spinning flow, the stress is obtained from the descent distance below the position in question specifically:

$$\sigma_1 - \sigma_2 = \left(4\sigma_{12}^2 + N_1^2\right) \qquad \text{(shear flow)}$$

$$(\sigma_1 - \sigma_2)(x_m) = \frac{1}{A(x_m)} \int_{x_m}^{L} \rho g\, A(x_1)\, dx_1 \qquad \text{(spinning flow)} \qquad \text{(14a, b)}$$

Our shear flow birefringence was measured in the '1-3' plane and is $(n_1 - n_3)$. Our elongational flow birefringence is $(n_1 - n_2)$.

The ratio of the birefringence in a solution of concentration ϕ_p^2

to that in a solution with concentration ϕ_{p1} at the same stress is

$$\frac{\Delta n(\phi_{p2})}{\Delta n(\phi_{p1})} = \frac{C(\phi_{p2})}{C(\phi_{p1})} \tag{15}$$

The stress optical constant for flexible chain systems should be proportional to the concentration of chains. We would expect the ratio of Eq (15) to be ϕ_{p2}/ϕ_{p1}. We find that if we compare values of $\Delta n(\phi_{p2}/\Delta n(\phi_{p1})$ for the liquid crystalline and isotropic solutions in this way, the ratio considerably exceeds ϕ_{p2}/ϕ_{p1}. The increase in orientation is associated with this is greater by an order of magnitude or more.

According to Oda, White and Clark, the value C/Δ° has the same value for polymer melts with flexible chains being approximately 0.2 x 10^5 Brewster (10^{-13} cm^2/dyne). The values we have found for the liquid crystalline solution

$$\frac{C}{\phi_p \Delta^\circ} = \frac{\Delta n}{(\sigma_1 - \sigma_2)\phi_p \Delta^\circ} \tag{16}$$

considerably exceed this value. For the HPC the mean value of this ratio for anisotropic solutions is 700 x 10^5 Brewster, a factor 3500 greater. However, it is to be noted that the values for the isotropic HPC solutions also exceed the flexible polymer chain value with a mean value of 30 x 10^5 Brewster. This could be due to chain rigidity and uncertainties in $\phi_p \Delta^\circ$. (For shear flow we have presumed here $(n_1 - n_3) \sim (n_1 - n_2)$).

Due to the problems of evaluation $\phi_p \Delta^\circ$ we cannot critically discuss the PPD-T solutions in a similar manner though the same situation clearly arises.

It should be noted there is no experimental proof of the rheo-optical law for liquid crystalline polymer solutions. Indeed it might

be suspected that it should not be so. Certainly Figure 10 (b) suggests that the stress optical law is not valid in start-up or cessation of flow. It is to be noted that Brodnyan, Gaskins, Philippoff and Lendrat (79) have checked the validity of the rheo-optical law in shear flow of isotropic solutions of some cellulose derivatives (but not HPC).

CONCLUSIONS

We have presented an experimental study of the birefringent characteristics of isotropic and liquid crystalline solutions of hydroxy propyl cellulose (HPC) in H_2O and poly-p-phenylene terephthalamide (PPD-T) in H_2SO_4 in the quiescent state, in shear flow and in elongational 'spinning' flow.

(1) In the quiescent state, domain structures exist with macromolecules arranged tangentially around the circumference. The HPC solution is cholesteric possessing a superposed twist at a smaller scale.

(2) In shear flows, the domain structures of both completely anisotropic solutions break up at sufficiently high deformation rates and the fluid achieves a homogeneous highly oriented state. Orientation levels are much higher than in the isotropic fluids and decay away much more slowly.

(3) The cholesteric structure HPC solution transforms to an oriented nematic state in shear flow.

(4) Upon stoppage of flow, the domain structure reforms and HPC regains its cholesteric character.

(5) In elongational flow, no domain structures are observed and much higher orientation levels are obtained than shear flow when comparisons are made at either the same deformation rate or differences

in principal stresses.

ACKNOWLEDGMENT

This work was supported in part by the U.S. Office of Naval Research.

APPENDIX 1

Determination of Intrinsic Birefringence From Bond Polarizabilities

Let the polarizabilities of individual bonds be α_{11}^i along their length and $a_{\perp}^i$ perpendicular to them (35, 36). We must now recognize that polarizability is a second order tensor (It relates the electrical field strength vector to the polarization vector) (31). The component α_{st}^i in the coordinate reference frame with axes along and perpendicular to the chain backbone are related to those in the coordinate frame of the bond α_{ab}^i by

$$\alpha_{st}^i = \sum_a \sum_b \ell_{sa}^i \ell_{tb}^i \alpha_{ab}^i \qquad \text{(A-1)}$$

where the ℓ_{sp}^i are cosines of the angles between the axes defining the ith bond and the extended macromolecule. For a structural unit with n bonds

$$\alpha_{st} = \sum_i \alpha_{st}^i = \sum_i^n \sum_a \sum_b \ell_{sa}^i \ell_{tb}^i \alpha_{ab}^i \qquad \text{(A-2)}$$

Introducing the matrix representation of α_{ab}^i in the bond:

$$\underset{\sim}{\alpha}^i = \begin{vmatrix} \alpha_b^i & 0 & 0 \\ 0 & \alpha_{pb}^i & 0 \\ 0 & 0 & \alpha_{pb}^i \end{vmatrix} \qquad \text{(A-3)}$$

Here α_b^i is along bond i and α_{pb}^i is perpendicular to bond i.

We may write the components α_{st} as

$$\alpha_{11} = \sum_i^n [\alpha_b^i \cos^2\theta_{11}^i + \alpha_{pb}^i (\cos^2\theta_{12}^i + \cos^2\theta_{13}^i)]$$

$$= \sum_i^n [\alpha_b^i \cos^2\theta_{11}^i + \alpha_{pb}^i \sin^2\theta_{12}^i] \qquad \text{(A-4a)}$$

$$\alpha_{22} = \sum_i^n [\alpha_b^i \cos^2\theta_{21}^i + \alpha_{pb}^i (\cos^2\theta_{22}^i + \cos^2\theta_{23}^i)]$$

$$= \sum_i^n [\alpha_b^i \sin^2\theta_{11}^i \cos^2\phi^i + \alpha_{pb}^i (\sin^2\theta^i \cos^2\phi_{11}^i \cos^2\theta)] \qquad \text{(A-4b)}$$

$$\alpha_{33} = \sum_i^n [\alpha_b^i \sin^2\theta_{11}^i \sin^2\theta^i + \alpha_{pb}^i (\cos^2\theta^i + \cos^2\theta_{11}^i \sin^2\phi^i)] \qquad \text{(A-4c)}$$

where ϕ^i is the azimuthal angle between the 2 axis in the chain coordinate frame and the longitude defined by the ith bond axis. α_{11} and $\alpha_{\perp}$ are given by

$$\alpha_{11} = \alpha_{11} \qquad \alpha_{\perp} = \frac{1}{2}(\alpha_{22} + \alpha_{33}) \qquad \text{(A-5)}$$

(Compare the discussions of Gurnee (35) and Kawai and his coworkers (80, 81).

APPENDIX 2

Calculation of Intrinsic Birefringence for PPD-T

Using the bond positions of the (orthorhombic) crystalline lattice structures of PPD-T as given by Northolt (82) (See Figure 17) we have computed α_{11}, α_{22} and α_{33} as well as n_a, n_b, n_g and $\Delta°$ for PPD-T. We obtain in terms of Northolts orthorhombic unit cell with Bunn and Daubeny's bond polarizabilities (36)

$$\alpha_\gamma = \alpha_{11} = 321.6 \times 10^{-25} cm^3$$

$$\alpha_\beta = \alpha_{22} = 268.4 \times 10^{-25} cm^3$$

$$\alpha_\alpha = \alpha_{33} = 195.0 \times 10^{-25} cm^3$$

$$n_\gamma = 2.038 \qquad n_\beta = 1.803 \qquad n_\alpha = 1.537$$

γ, β, and α correspond to the c, b and a crystallographic directions. This leads to

$$\alpha = \alpha_\gamma \qquad \alpha_\perp = 232 \times 10^{-25} cm^3 \qquad \Delta° = 0.368$$

This calculation neglects complexities due to the internal field (33) presumes the density of the crystal and neglects form birefringence (31, 32, 40-44).

APPENDIX 3

Calculation of Intrinsic Birefringence for HPC

Hydroxypropyl cellulose is a more difficult polymer to characterize because of uncertainity of the configurations of the substituent groups. (See Figure 18) For cellulose itself, we may readily make calculations. These have been most recently done by Takahara et al (81) who have used the atomic arrangements of Meyer and Misch (83) for the cellulose II crystalline form and the Bunn-Daubeny bond polarizabilities (36). This is more awkward because the unit cell is monoclinic rather than orthorhombic. They obtain

α_γ (b-axis) = $147.0 \times 10^{-25} cm^3$

α_β (parallel to pyranose ring normal to 101 plane) - $142.2 \times 10^{-25} cm^3$

α_α (normal to pyranose ring, parallel to 101 plane) - $119.2 \times 10^{-25} cm^3$

$\alpha_{11} = \alpha_\gamma$ $\qquad$ $\alpha_\perp = 133.7 \times 10^{-25} cm^3$

$n_\gamma = 1.650$ which leads to

$n_\beta = 1.624$ $\qquad$ $n_\alpha = 1.504$

$\Delta^\circ = 0.086$

The presence of the propylene oxide ether groups should certainly lower α_α, n_α, and Δ°. The crystal structure of HPC has been studied by Samuels (37) who finds it to be rather complex (Figure 18) with the pyranose ring twisted relative to each other and part of the propylene oxide chains being parallel to the axis (thus affecting α_γ). Samuels also records experimental data for density and calorimetric crystallinity, birefringence

and amorphous, f_a, and crystalline, f_c, orientation factors in partially oriented films. These are interrelated through Hermans equation (84) (see also Taylor and Darin (85) and Stein and Norris (86):

$$\Delta n = X f_c \Delta^\circ_c + (1 - X) f_a \Delta^\circ_a \qquad \text{(C-1)}$$

From this we compute

$$\Delta^\circ = \Delta^\circ c = 0.038$$

with Δ°_a of 0.019.

REFERENCES

1. C. Robinson, Trans Faraday Soc., 52, 571 (1956).

2. C. Robinson, J. C. Ward, and R. B. Beevers, Disc. Faraday Soc., 25, 29 (1958).

3. C. Robinson, Tetrahedron, 13, 219 (1961).

4. W. G. Miller, C. C. Wu, E. L. Wee, G. L. Santee, J. H. Rai and K. G. Goebel, Pure Appl. Chemistry, 43, 37 (1974).

5. E. T. Samulski and A. J. Tobolsky in "Liquid Crystals and Plastic Crystals" edited by G. Gray and P. Winsor, Wiley, NY (1974).

6. T. Asada, Y. Maruhashi, Y. Kuroki and S. Onogi, J. Soc. Rheol., Japan, 6, 14 (1978).

7. T. Asada, H. Muramatsu and S. Onogi, J. Soc. Rheol., Japan, 6, 130 (1978).

8. H. Aoki, J. L. White and J. F. Fellers, J. Appl. Polym. Sci., 23, 2293 (1979).

9. Y. Onogi, J. L. White and J. F. Fellers, J. Polym. Sci., Polym. Phys. (in press).

10. S. L. Kwolek, U.S. Patent 3,671,542 (1972).

11. P. W. Morgan, Macromolecules, 10, 1381 (1977).

12. S. L. Kwolek, P. W. Morgan, J. R. Schaefgen and L. W. Gulrich, Macromolecules, 10, 1390 (1977).

13. T. I. Bair, P. W. Morgan and F. L. Killian, Macromolecules, 10, 1396 (1977).

14. T. A. Hancock, J. E. Spruiell and J. L. White, J. Appl. Polym. Sci., 21, 1227 (1977).

15. M. Horio, Ann. Report Res. Inst. Chem. Fibers, 35, (Oct) 87 (1978).

16. H. Aoki, Y. Onogi, J. L. White and J. F. Fellers, Polym. Eng. Sci., (in press).

17. W. J. Jackson and H. F. Kuhfuss, J. Polym. Sci., Polym. Chem., 14, 2043 (1976).

18. T. C. Pletcher, U.S. Patent 3,991,013 (1976).

19. J. J. Kleinschuster, U.S. Patent 3,991,014 (1976).

20. W. R. Krigbaum and F. Salaris, J. Polym. Sci., Polym. Phys., 16, 883 (1978).

21. D. G. Baird, J. Appl. Polym. Sci., 23, 941 (1979).

22. R. S. Werbowyj and D. G. Grey, Mol. Cryst. Liq. Cryst. (Letters) 34, 47 (1976).

23. M. Panar and O. Burr, Offenlegungsschrift 2705382, West Germany (1977).

24. T. Asada, Papers presented at the Society of Rheology, Japan Meeting, October (1978).

25. P. J. Flory, Proc. Roy. Soc., A234, 73 (1956), J. Polym. Sci., 49, 105 (1961).

26. P. J. Flory and A. Abe, Macromolecules, 11, 1119, 1122, 1138, 1141, (1978).

27. J. L. White and J. F. Fellers, "Fiber Structure and Properties," edited by J. L. White, Appl. Polym. Symp., 33, 137 (1978).

28. P. H. Hermans and P. Platzek, Kolloid Z, 88, 68 (1939) and J. J. Hermans, P. H. Hermans, D. Vermaas and A. Weidinger, Rec. Trav. Chim., 65, 427 (1946).

29. H. A. Lorentz, "Theory of Electrons," 2nd ed., Dover reprint of 1915 edition (1952).

30. L. Page and N. I. Adams, "Electrodynamics," Van Nostrand, NY (1940).

31. M. Born and E. Wolf, "Principles of Optics," 4th ed. Pergamon London (1970).

32. Lord Rayleigh, Phil. Mag, (5), 34, 481 (1892).

33. R. S. Stein, J. Polym. Sci., A-2, 7, 1021 (1969).

34. W. Kuhn and F. Grun, Kolloid Z, 101, 248 (1942).

35. E. F. Gurnee, J. Appl. Phys., 25, 1232 (1954).

36. C. W. Bunn and R. De P. Daubeny, Trans. Faraday Soc., 50, 1173 (1954).

37. R. J. Samuels, J. Polym. Sci., A-2, 7, 1197 (1969).

38. L. Konopasek and J. W. S. Hearle, J. Appl. Polym. Sci., 21, 2791.

39. O. Wiener, Abh Sachs "Ges Akad Wiss Math Phys kl, No. 6, 32, 575 (1912).

40. W. L. Bragg and A. B. Pippard, Acta Cryst., 6, 865 (1953).

41. M. J. Folkes and A. Keller, Polymer 12, 222 (1971).

42. M. Copic, J. Chem. Phys., 26, 1382 (1957).

43. H. Janeschitz-Kriegl, Makromol. Chemie., 40, 140 (1960).

44. R. Koyama, J. Phys. Soc., Japan, 16, 1366 (1961).

45. B. D. Coleman and W. Noll, Arch. Rat. Mech. Anal., 3, 289 (1959).

46. B. D. Coleman and W. Noll, Phys. Fluids, 5, 840 (1962).

47. F. C. Frank, Disc. Faraday Soc., 25, 19 (1958).

48. J. L. Ericksen, Arch. Rat. Mech. Anal., 9, 371 (1962), J. Fluid Mech., 27, 59 (1967), Trans. Soc. Rheol., 11, 5 (1967).

49. F. M. Leslie, Arch. Rat. Mech. Anal., 28, 265 (1968).

50. F. M. Leslie, Mol. Cryst. Liq. Cryst., 7, 407 (1969).

51. J. L. Ericksen, Mol. Cryst. Liq. Cryst., 7, 153 (1969).

52. R. J. Atkin and F. M. Leslie, Q. J. Mech. Appl. Math., 23, 53 (1970).

53. R. J. Atkin, Arch. Rat. Mech. Anal., 38, 224 (1970).

54. J. E. Ericksen, Trans. Soc. Rheol., 13, 9 (1969).

55. R. S. Porter, E. M. Barrall and J. F. Johnson, J. Phys. Chem., 66, 1826 (1962).

56. J. Fisher and A. G. Fredricksen, Mol. Cryst. Liq. Cryst., 8, 267 (1969).

57. J. C. Maxwell, Proc. Roy. Soc., 22, 46 (1873).

58. J. T. Edsall in Advances in Colloid Science edited by E. O. Kraemer, Vol. 1, Interscience, NY (1942).

59. C. Tanford, "Physical Chemistry of Macromolecules," Wiley, NY (1961).

60. A. S. Lodge, Trans. Faraday Soc., 52, 120 (1956).

61. W. Philippoff, J. Appl. Phys., 27, 984 (1956).

62. J. G. Brodnyan, F. H. Gaskins and W. Philippoff, Trans. Soc. Rheol., 1, 107 (1957).

63. W. Philippoff, Proc. 4th Int. Rheological Cong., 2, 343 (1965).

64. W. Philippoff and E. G. M. Tornquist, J. Polym. Sci., C23, 881 (1968).

65. E. B. Adams, J. C. Whitehead and D. C. Bogue, AIChE J., 11, 1026 (1965).

66. H. Janeschitz-Kriegl, Adv. Polym. Sci., 6, 170 (1969).

67. R. S. Stein, Rubber Chem. Technol., 49, 458 (1976).

68. F. H. Gortemaker, H. Janeschitz-Kriegl and K. T. Nijenhuis, Rheol. Acta, 15, 487 (1976).

69. L. R. G. Treloar, "Trans. Faraday Soc., 43, 277 (1947).

70. L. R. G. Treloar, "Physics of Rubber Elasticity," 2nd ed., Oxford (1958).

71. K. Oda, J. L. White and E. S. Clark, Polym. Eng. Sci., 18, 53 (1978).

72. K. Walters, "Rheometry," Chapman and Hall, London (1975).

73. A. Saupe, in "Liquid and Plastic Crystals," Vol. 1 edited by G. W. Gray and P. A. Winsor, Horwood, Chichester (1974).

74. N. H. Hartshorne in "Liquid and Plastic Crystals," Vol. 2 edited by G. W. Gray and P. W. Winsor, Horwood, Chichester (1974).

75. J. L. Fergason, Mol. Cryst., 1, 293 (1966); J. L. Fergason, N. N. Goldberg and R. J. Radalin, ibid, 1, 309 (1966).

76. W. Haas, J. Adams, and J. Wysocki, Mol. Cryst. Liq. Cryst., 7, 395 (1969).

77. S. Kusabayashi and M. M. Labes, Mol. Cryst. Liq. Cryst., 7, 395 (1969).

78. J. D. Bernal and I. Fankuchen, J. Gen Physiol, 25, 111 (1941).

79. J. G. Broonyan, F. H. Gaskins, W. Philippoff and E. G. Lendrat, Trans. Soc. Rheol., 2, 285 (1958).

80. S. Nomura, H. Kawai, I. Kimura and M. Kagiyama, J. Polym. Sci., A-2, 5, 479 (1967).

81. H. Takahara, S. Nomura, H. Kawai, Y. Yamaguchi, K. Okazaki and A. Fukushima, J. Polym. Sci., A-2, 6, 197 (1968).

82. M. G. Northolt, European Polym. J., 10, 799 (1974).

83. K. H. Meyer and L. Misch, Helv Chim. Acta, 20, 232 (1937).

84. P. H. Hermans, J. J. Hermans, D. Vermaas and A. Weidineer, J. Polym. Sci., 3, 1 (1948).

85. G. R. Taylor and S. R. Darin, J. Appl. Phys., 26, 1075 (1955).

86. R. S. Stein and F. H. Norris, J. Polym. Sci., 21, 381 (1956).

FIGURE 1. LATTICE MODEL FOR THE FORMATION OF POLYMER LIQUID CRYSTALS.

FIGURE 2. RELATIVE TRANSMITTED LIGHT INTENSITY THROUGH CROSSED POLARS WHERE I_0 IS LIGHT INTENSITY WHEN THE SOLUTION IS ISOTROPIC. SAMPLE THICKNESS IS 100 μ.

FIGURE 3. POLARIZED LIGHT PHOTO MICROGRAPHS OF PPD-T SOLUTIONS.

A. SMALL SPHERULITES AND THEIR AGGREGATES AT 9.2% PPD-T IN 100% H_2SO_4.

B. 11% PPD-T SOLUTION BEFORE ANNEALING.

C. 11% PPD-T SOLUTION AFTER HEATING TO 90°C AND COOLING TO AMBIENT TEMPERATURE.

FIGURE 4. POLARIZED LIGHT PHOTOMICROGRAPHS OF HPC SOLUTIONS.

A. AGGREGATES OF ANISOTROPIC HPC PARTICLES AT 42 WT.% HPC IN WATER.

B. SPHERULITIC STRUCTURE AT 70 WT. % HPC/30% WATER.

FIGURE 5. ARRANGEMENT OF PPD-T AND HPC MACROMOLECULES IN NEGATIVE SPHERULITES.

FIGURE 6. ABSORPTION SPECTRA OF HPC ANISOTROPIC SOLUTIONS WHOSE CONCENTRATIONS RANGE FROM 56.7 WT. % TO 70 WT. %. SAMPLES THICKNESS IS 100 MICRONS.

FIGURE 7. SCHEMATIC REPRESENTATION OF POLYMER CHAIN ORIENTATION IN CHOLESTERIC LIQUID CRYSTALS.

FIGURE 8. STRUCTURAL ARRANGEMENTS EXPLAINING SAMPLE SIZE EFFECTS IN HPC SOLUTIONS.

FIGURE 9. TRANSIENT BUILDUP OF SHEAR STRESS IN HPC SOLUTIONS.

A. 45 WT. % HPC IN WATER.

B. 55 WT. % HPC IN WATER.

FIGURE 10. A. THE BIREFRINGENCE AND STRESS RESPONSES OF AN ISOTROPIC 30% HPC SOLUTION PLOTTED AGAINST FLOW TIME. THE SUBSCRIPT 'ST' REFERS TO THE STEADY FLOW CONDITION.

B. THE BIREFRINGENCE AND STRESS RESPONSES OF AN ANISOTROPIC 55% HPC SOLUTION PLOTTED AGAINST FLOW TIME. THE SUBSCRIPT 'ST' REFERS TO THE STEADY FLOW CONDITION.

FIGURE 11. BIREFRINGENCE RELAXATION FOLLOWING CESSATION OF FLOW FOR HPC SOLUTIONS.

A. 45 WT. % HPC IN WATER.

B. 55 WT. % HPC IN WATER.

FIGURE 12. STEADY STATE BIREFRINGENCE FOR HPC SOLUTIONS AS A FUNCTION OF CONCENTRATION AND SHEAR RATE.

FIGURE 13. STEADY STATE BIREFRINGENCE AS A FUNCTION OF CONCENTRATION AND SHEAR RATE FOR PPD-T SOLUTIONS.

FIGURE 14. PROPOSED FLOW INDUCED DOMAIN DEFORMATION AND DISAPPEARANCE MECHANISM OF POLYMER LIQUID CRYSTALS.

FIGURE 15. VELOCITY PROFILES ALONG THE SPINLINE FOR HPC SOLUTIONS.

FIGURE 16. A. BIREFRINGENCE AS A FUNCTION OF DESCENT DISTANCE ALONG THE ISOTROPIC HPC SPINLINE.

B. BIREFRINGENCE AS A FUNCTION OF SPINLINE POSITION FOR ANISOTROPIC HPC SOLUTION.

FIGURE 17. CRYSTAL STRUCTURE AND MOLECULAR ARRANGEMENT OF PPD-T AFTER NORTHOLT (82).

FIGURE 18. PROPOSED CRYSTALLINE MOLECULAR ARRANGEMENT OF HPC AFTER SAMUELS (37).

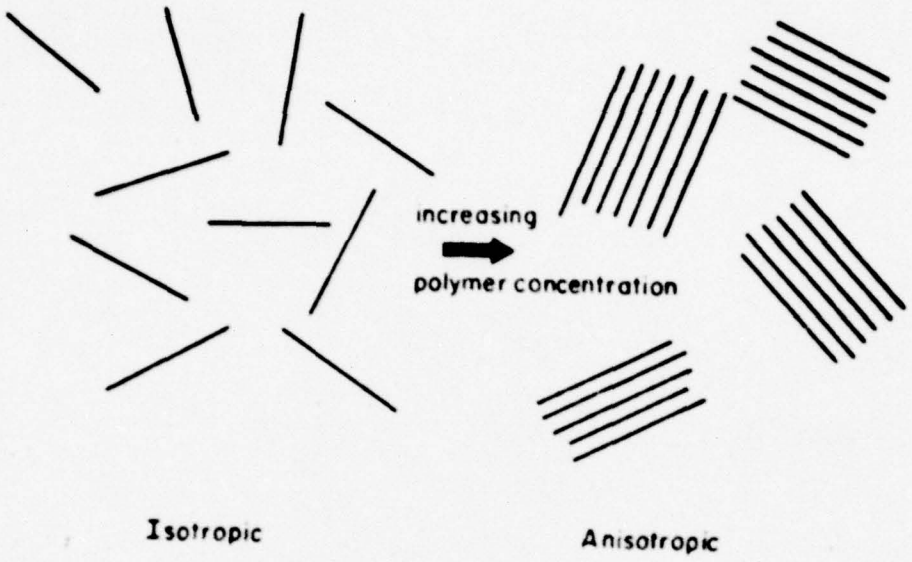

FIGURE 1. LATTICE MODEL FOR THE FORMATION OF POLYMER LIQUID CRYSTALS.

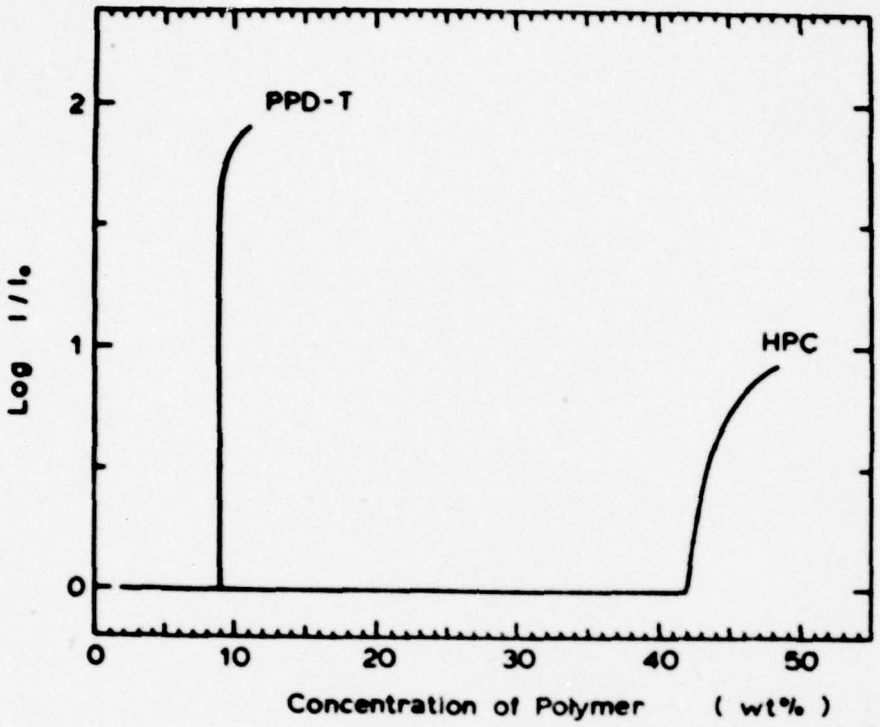

FIGURE 2. RELATIVE TRANSMITTED LIGHT INTENSITY THROUGH CROSSED POLARS WHERE I_0 IS LIGHT INTENSITY WHEN THE SOLUTION IS ISOTROPIC. SAMPLE THICKNESS IS 100 μ.

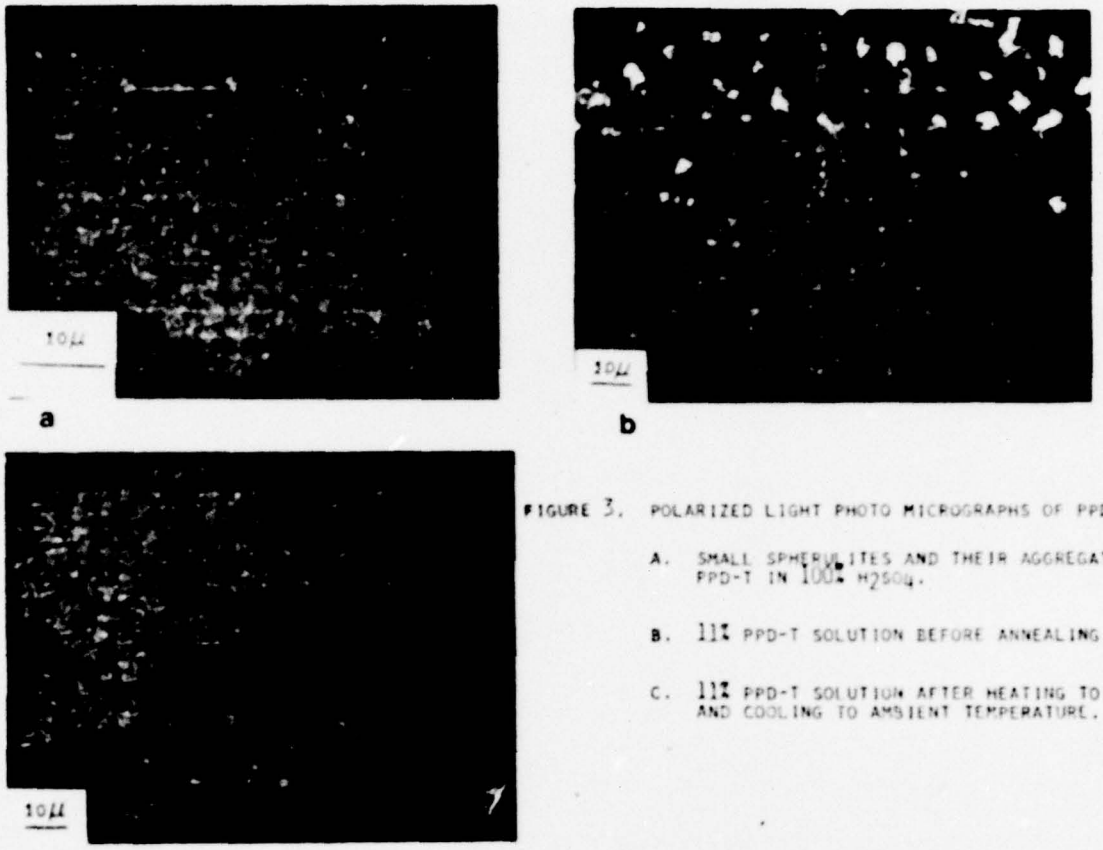

FIGURE 3. POLARIZED LIGHT PHOTO MICROGRAPHS OF PPD-T SOLUTIONS.

A. SMALL SPHERULITES AND THEIR AGGREGATES AT 9.2% PPD-T IN 100% H_2SO_4.

B. 11% PPD-T SOLUTION BEFORE ANNEALING.

C. 11% PPD-T SOLUTION AFTER HEATING TO 90°C AND COOLING TO AMBIENT TEMPERATURE.

a

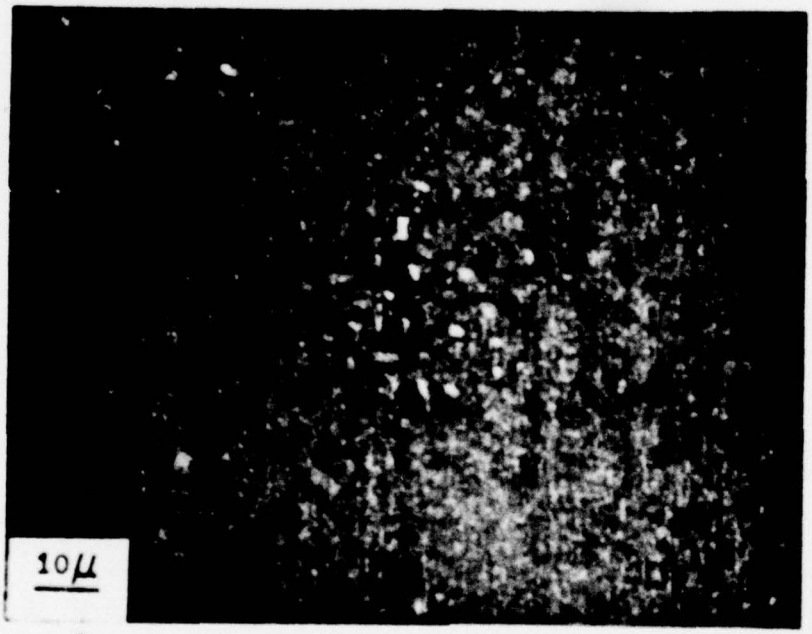

b

FIGURE 4. POLARIZED LIGHT PHOTOMICROGRAPHS OF HPC SOLUTIONS.

A. AGGREGATES OF ANISOTROPIC HPC PARTICLES AT 42 WT.% HPC IN WATER.

B. SPHERULITIC STRUCTURE AT 70 WT. % HPC/30% WATER.

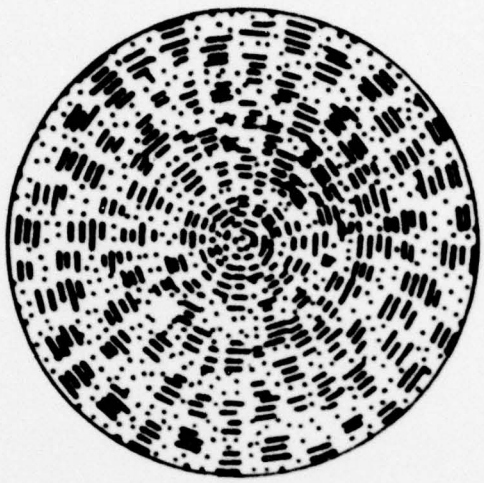

FIGURE 5. ARRANGEMENT OF PPD-T AND HPC MACROMOLECULES IN NEGATIVE SPHERULITES.

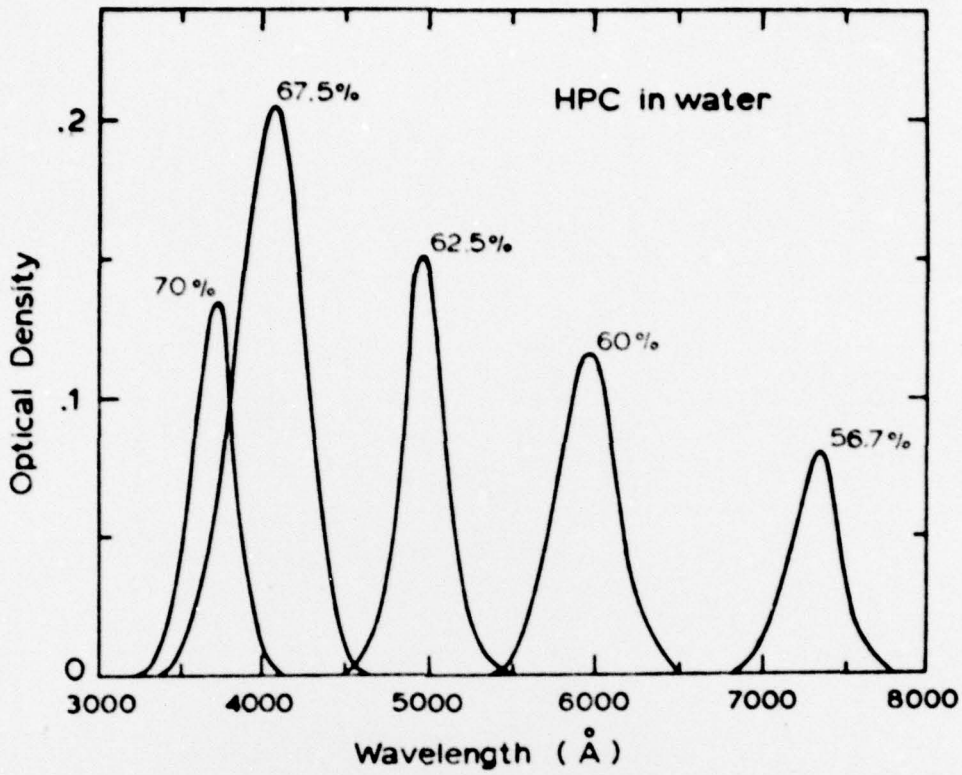

FIGURE 6. ABSORPTION SPECTRA OF HPC ANISOTROPIC SOLUTIONS WHOSE CONCENTRATIONS RANGE FROM 56.7 WT. % TO 70 WT. %. SAMPLES THICKNESS IS 100 MICRONS.

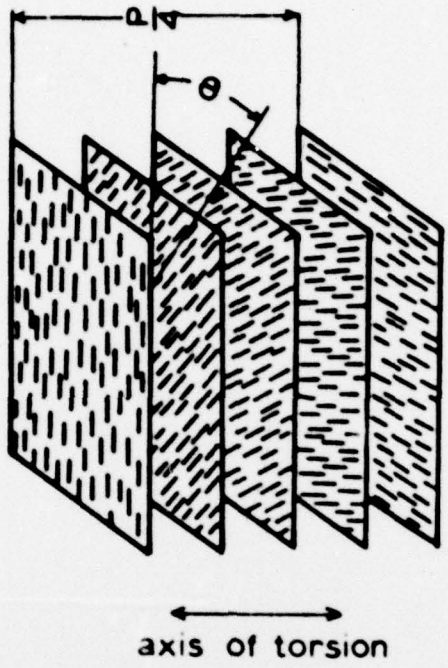

FIGURE 7. SCHEMATIC REPRESENTATION OF POLYMER CHAIN ORIENTATION IN CHOLESTERIC LIQUID CRYSTALS.

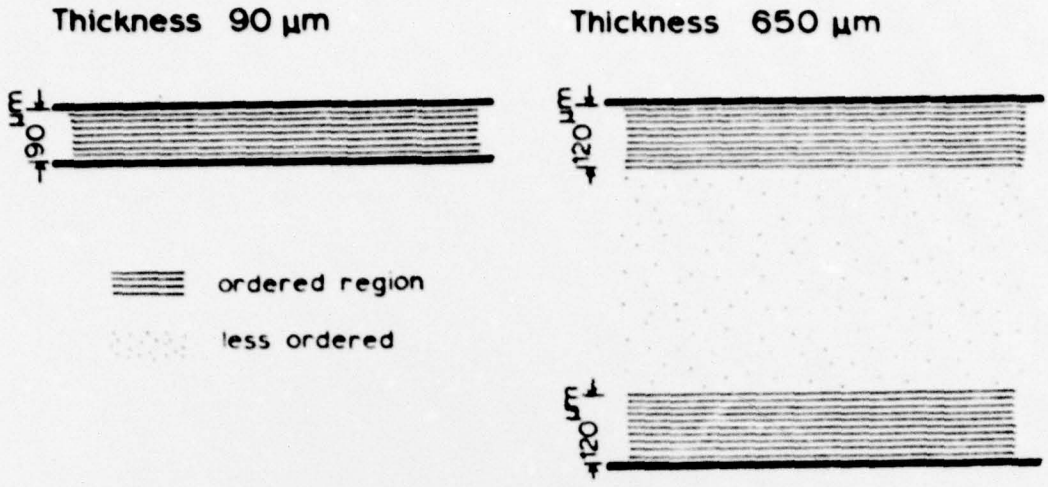

FIGURE 8. STRUCTURAL ARRANGEMENTS EXPLAINING SAMPLE SIZE EFFECTS IN HPC SOLUTIONS.

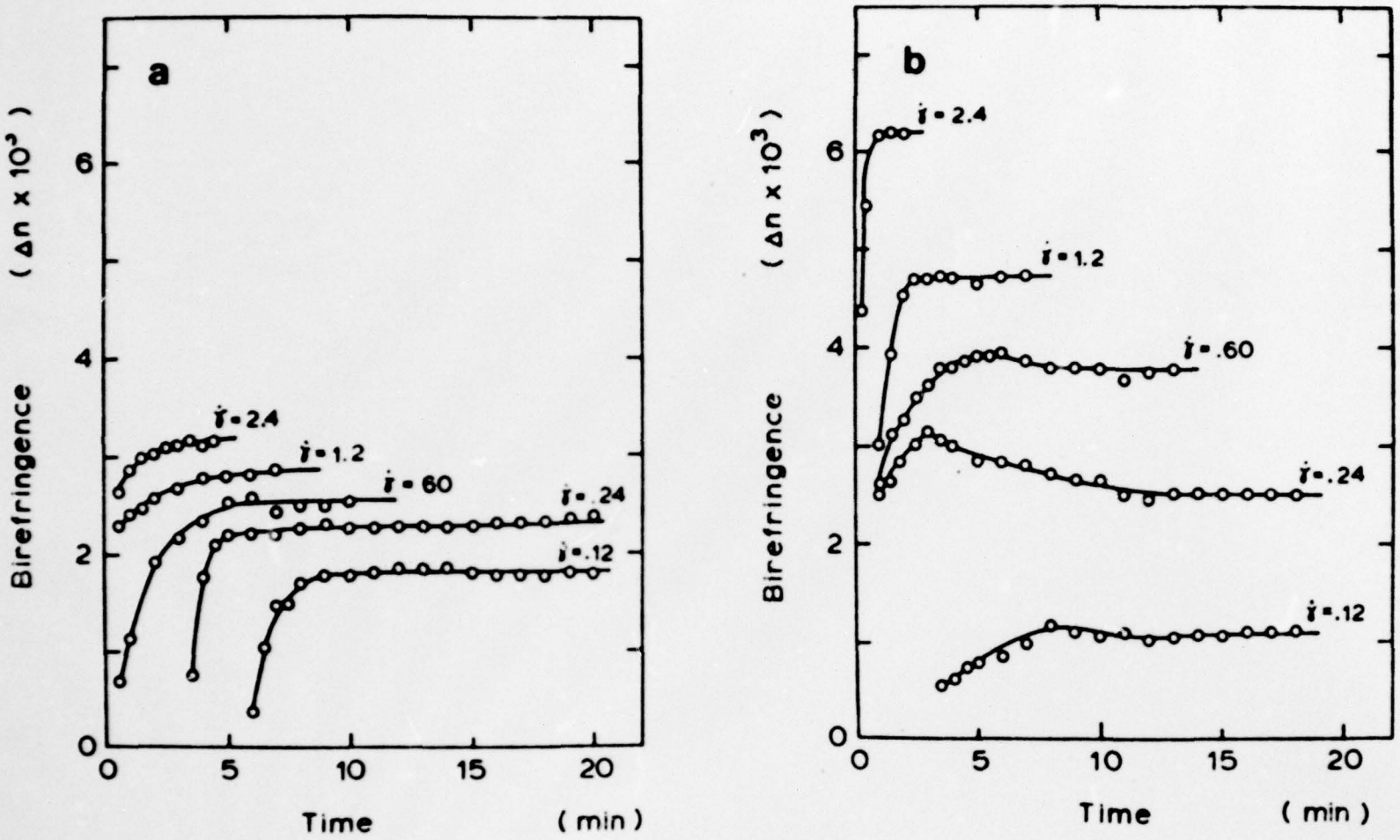

FIGURE 9. TRANSIENT BUILDUP OF SHEAR STRESS IN HPC SOLUTIONS.

A. 45 WT. % HPC IN WATER.

B. 55 WT. % HPC IN WATER.

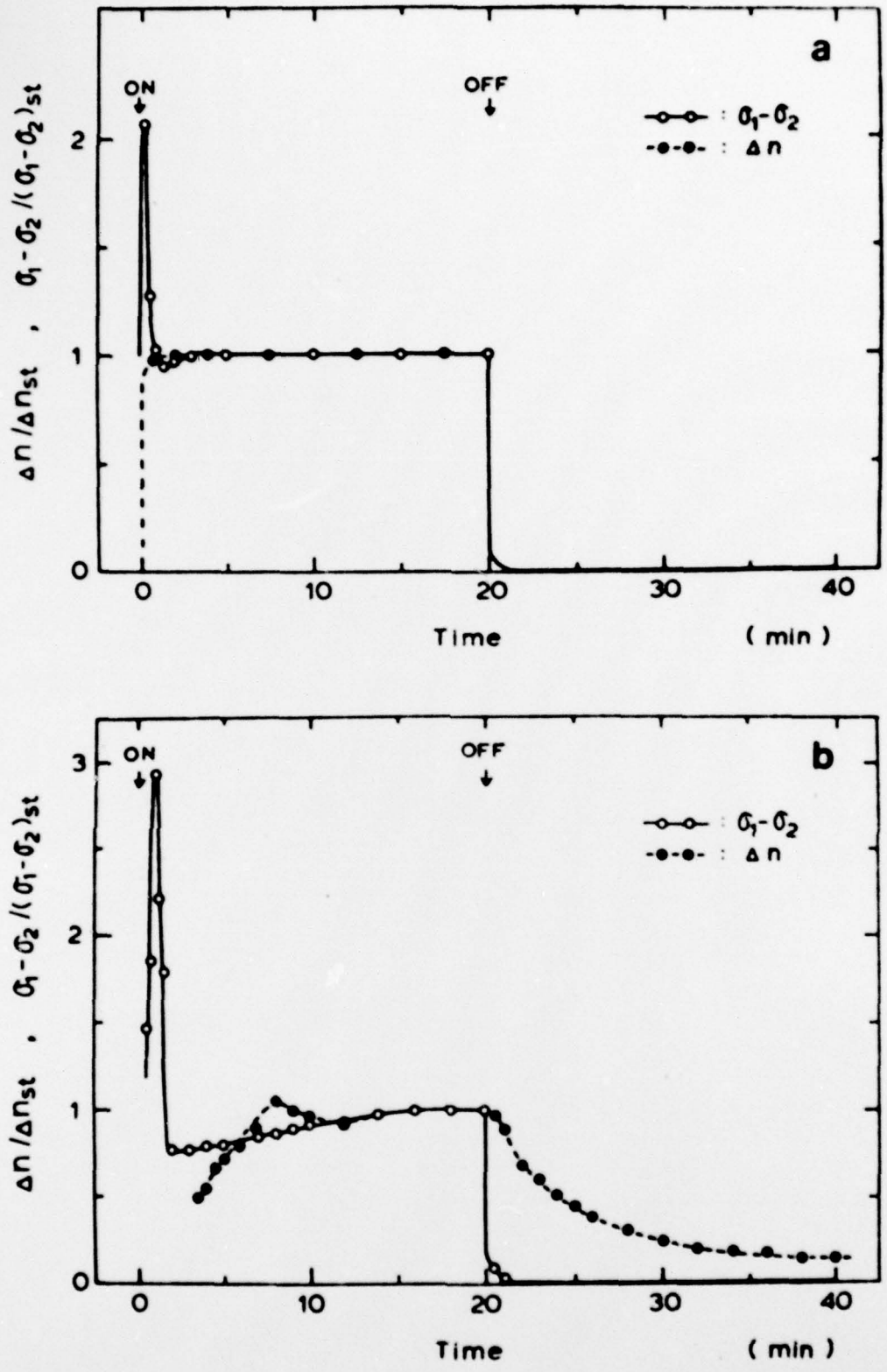

FIGURE 10. A. THE BIREFRINGENCE AND STRESS RESPONSES OF AN ISOTROPIC 30% HPC SOLUTION PLOTTED AGAINST FLOW TIME. THE SUBSCRIPT 'ST' REFERS TO THE STEADY FLOW CONDITION.

B. THE BIREFRINGENCE AND STRESS RESPONSES OF AN ANISOTROPIC 55% HPC SOLUTION PLOTTED AGAINST FLOW TIME. THE SUBSCRIPT 'ST' REFERS TO THE STEADY FLOW CONDITION.

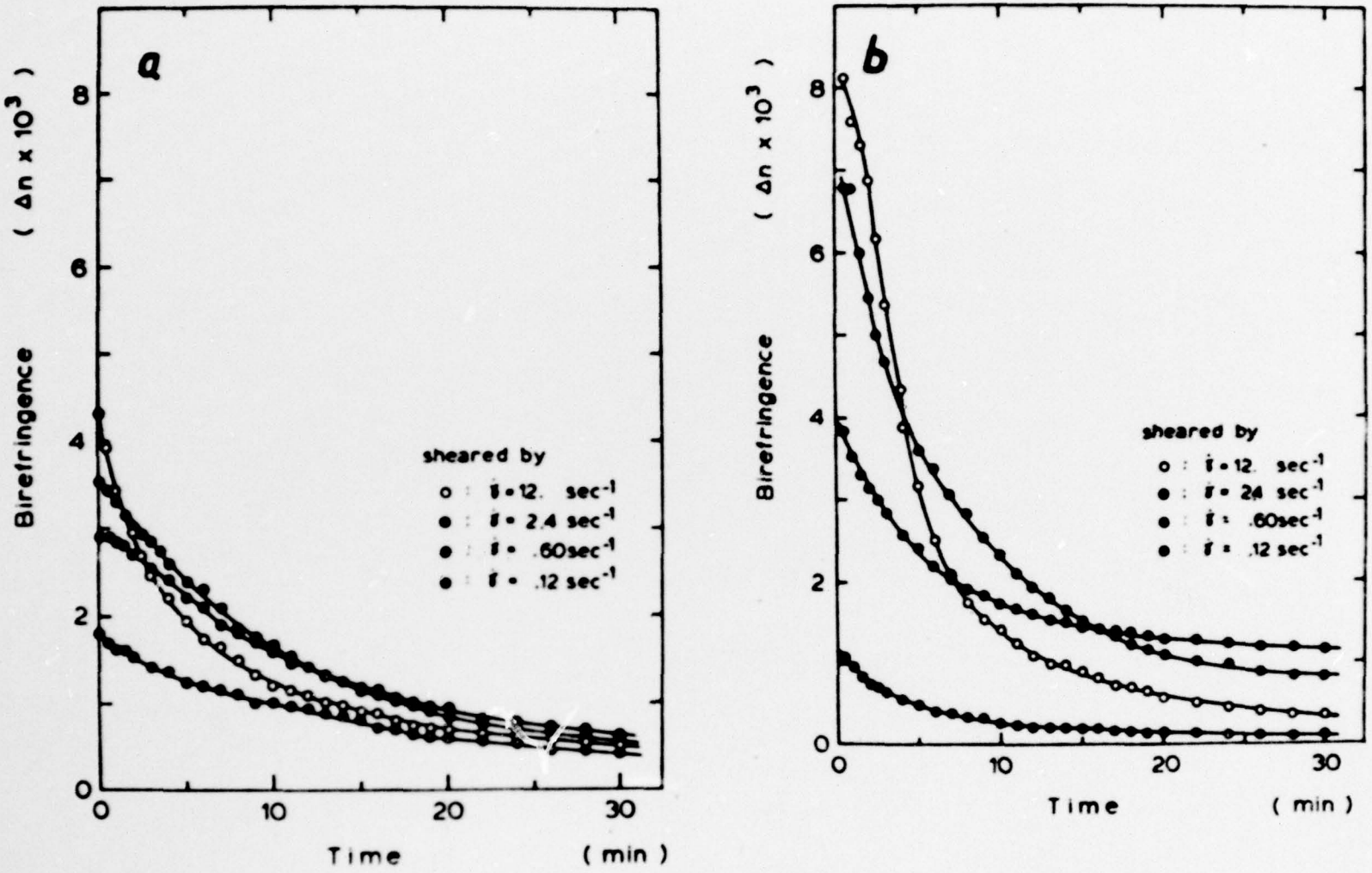

FIGURE 11. BIREFRINGENCE RELAXATION FOLLOWING CESSATION OF FLOW FOR HPC SOLUTIONS.

A. 45 WT. % HPC IN WATER.

B. 55 WT. % HPC IN WATER.

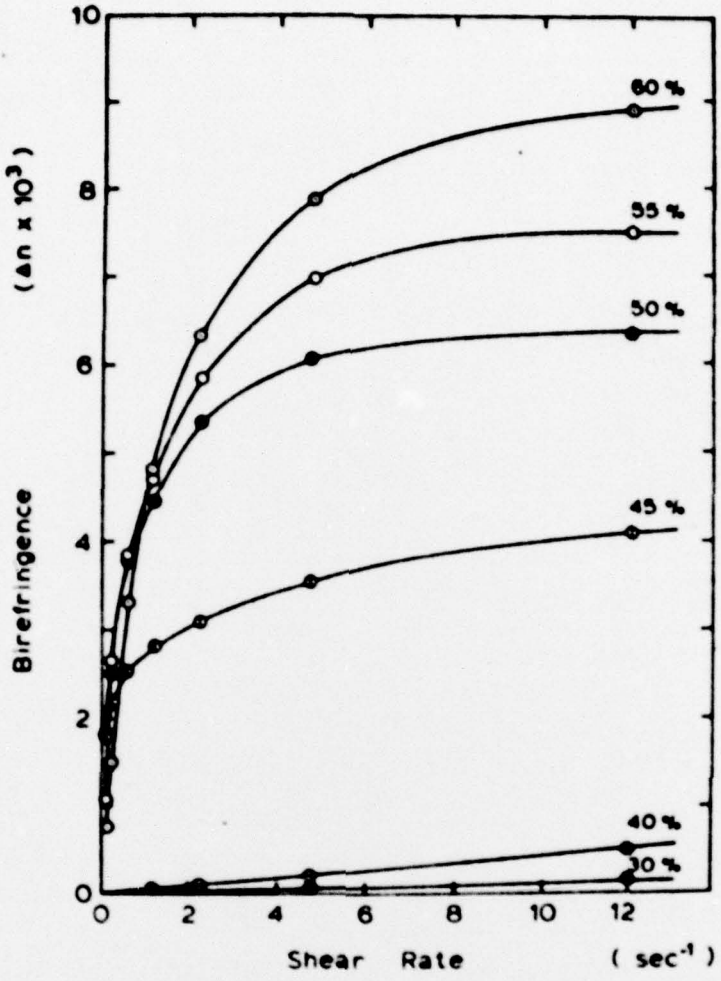

FIGURE 12. STEADY STATE BIREFRINGENCE FOR HPC SOLUTIONS AS A FUNCTION OF CONCENTRATION AND SHEAR RATE.

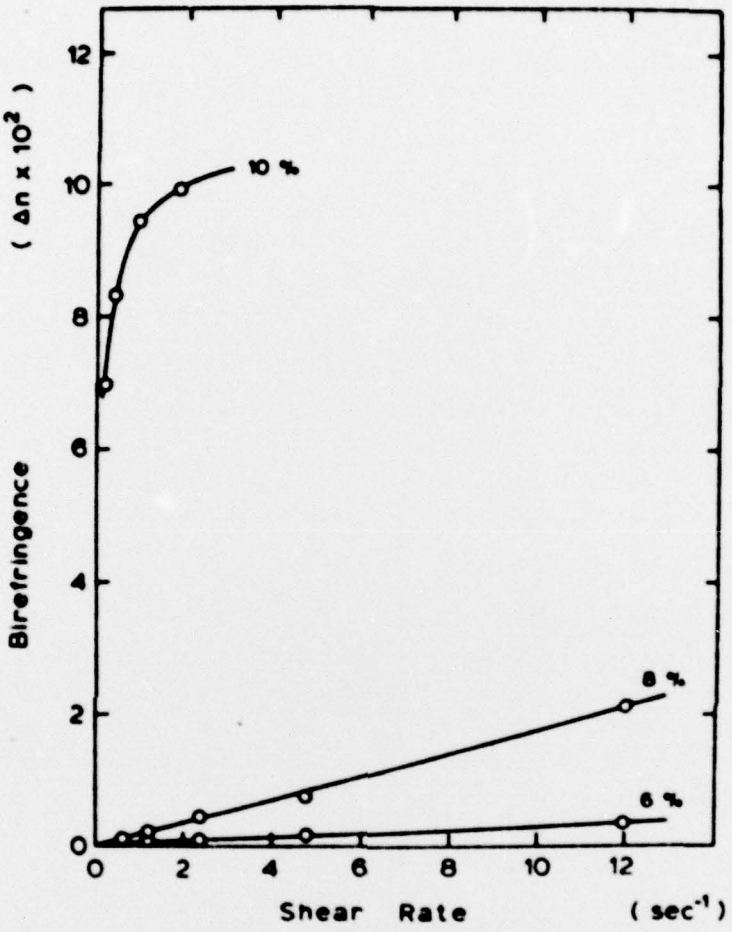

FIGURE 13. STEADY STATE BIREFRINGENCE AS A FUNCTION OF CONCENTRATION AND SHEAR RATE FOR PPD-T SOLUTIONS.

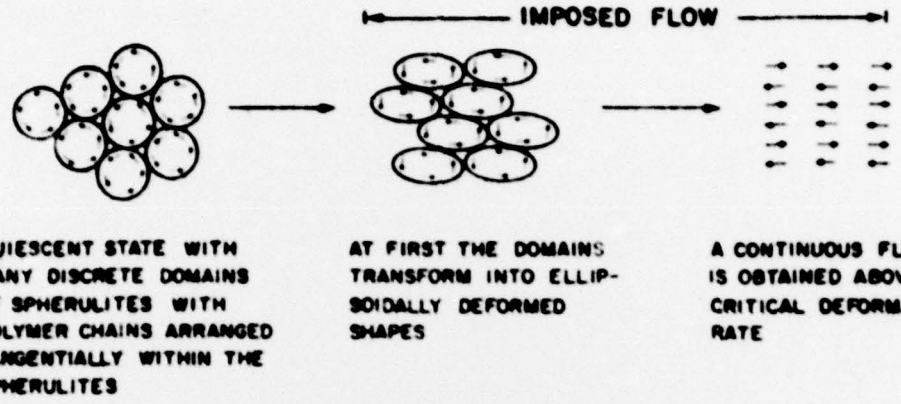

FIGURE 14. PROPOSED FLOW INDUCED DOMAIN DEFORMATION AND DISAPPEARANCE MECHANISM OF POLYMER LIQUID CRYSTALS.

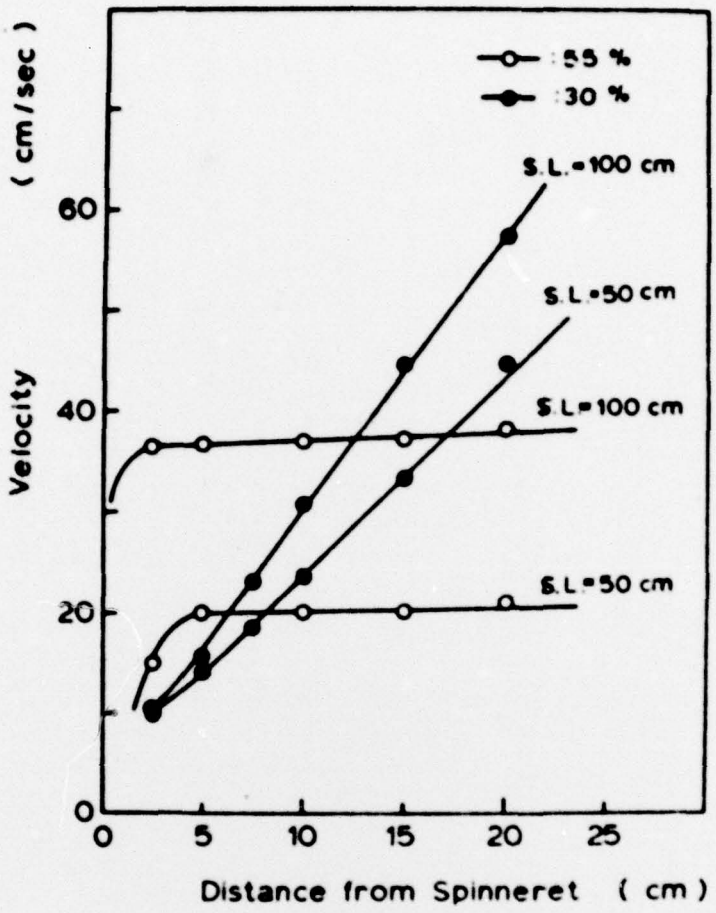

FIGURE 15. VELOCITY PROFILES ALONG THE SPINLINE FOR HPC SOLUTIONS.

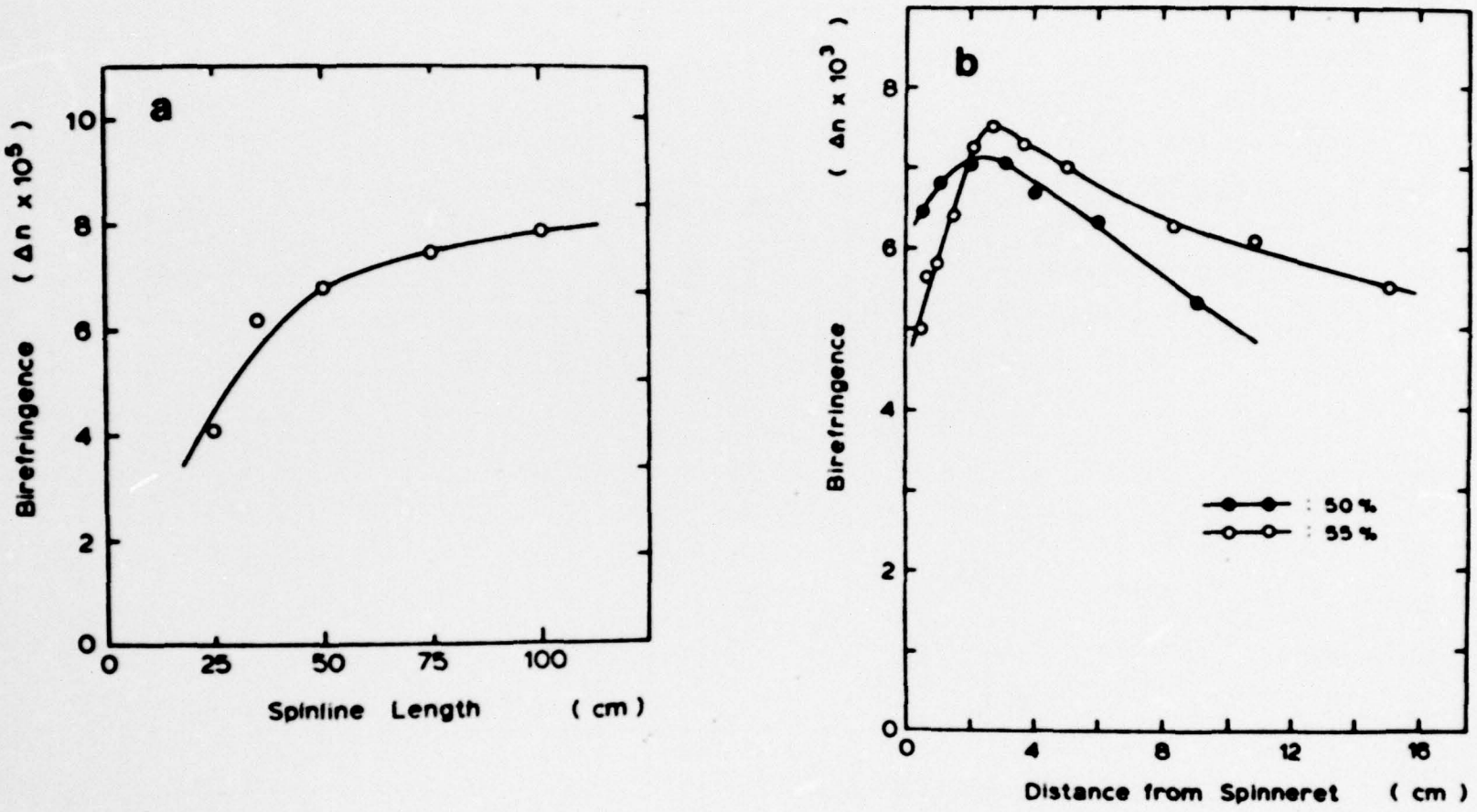

FIGURE 16. A. BIREFRINGENCE AS A FUNCTION OF DESCENT DISTANCE ALONG THE ISOTROPIC HPC SPINLINE.

B. BIREFRINGENCE AS A FUNCTION OF SPINLINE POSITION FOR ANISOTROPIC HPC SOLUTION.

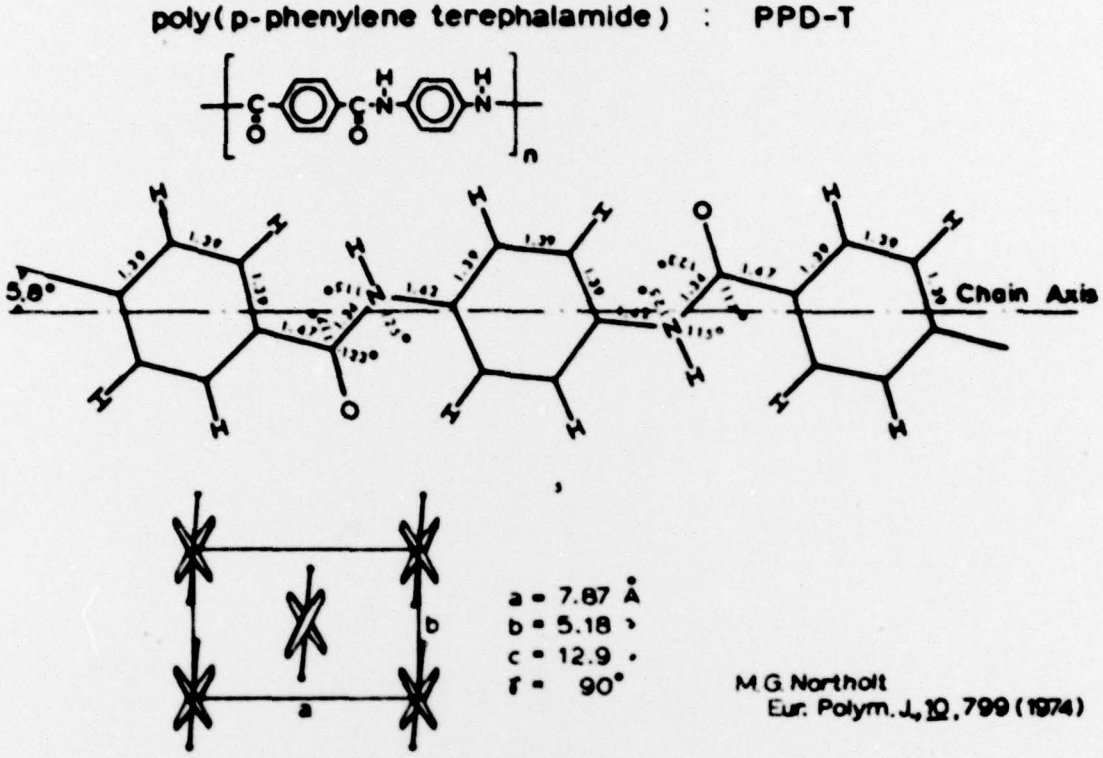

FIGURE 17. CRYSTAL STRUCTURE AND MOLECULAR ARRANGEMENT OF PPD-T AFTER NORTHOLT (82).

Idealized structure of hydroxypropylcellulose (HPC)

molecular substitution : 4

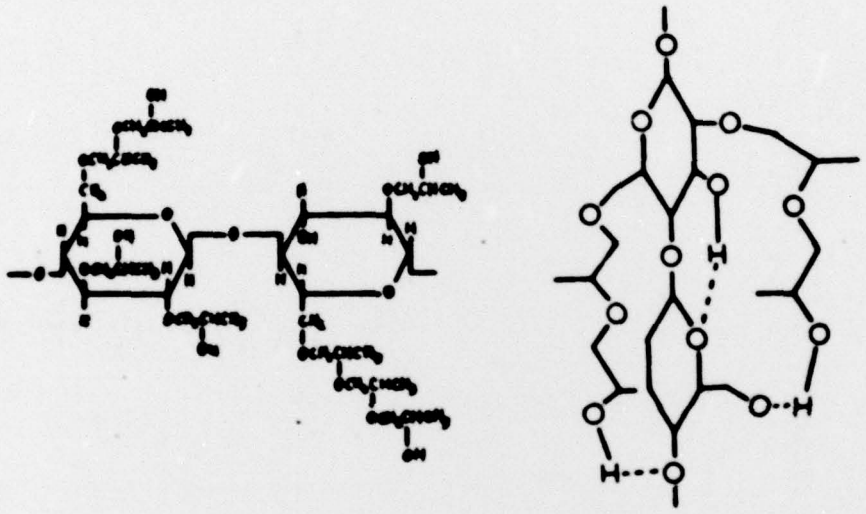

FIGURE 18. PROPOSED CRYSTALLINE MOLECULAR ARRANGEMENT OF HPC AFTER SAMUELS (37).